



THE UNIVERSITY *of* EDINBURGH

## Edinburgh Research Explorer

### How much (ATP) does it cost to build a trypanosome?

**Citation for published version:**

Nascimento, JF, Souza, ROO, Alencar, MB, Marsiccobetre, S, Murillo, AM, Damasceno, FS, Girard, RBMM, Marchese, L, Luévano-Martinez, LA, Achjian, RW, Haanstra, JR, Michels, PAM & Silber, A 2023, 'How much (ATP) does it cost to build a trypanosome? A theoretical study on the quantity of ATP needed to maintain and duplicate a bloodstream-form Trypanosoma brucei cell', *PLoS Pathogens*, vol. 19, no. 7, e1011522. <https://doi.org/10.1371/journal.ppat.1011522>

**Digital Object Identifier (DOI):**

[10.1371/journal.ppat.1011522](https://doi.org/10.1371/journal.ppat.1011522)

**Link:**

[Link to publication record in Edinburgh Research Explorer](#)

**Document Version:**

Publisher's PDF, also known as Version of record

**Published In:**

PLoS Pathogens

**General rights**

Copyright for the publications made accessible via the Edinburgh Research Explorer is retained by the author(s) and / or other copyright owners and it is a condition of accessing these publications that users recognise and abide by the legal requirements associated with these rights.

**Take down policy**

The University of Edinburgh has made every reasonable effort to ensure that Edinburgh Research Explorer content complies with UK legislation. If you believe that the public display of this file breaches copyright please contact [openaccess@ed.ac.uk](mailto:openaccess@ed.ac.uk) providing details, and we will remove access to the work immediately and investigate your claim.



## RESEARCH ARTICLE

# How much (ATP) does it cost to build a trypanosome? A theoretical study on the quantity of ATP needed to maintain and duplicate a bloodstream-form *Trypanosoma brucei* cell

Janaina F. Nascimento<sup>1</sup>, Rodolpho O. O. Souza<sup>1</sup>, Mayke B. Alencar<sup>1</sup>, Sabrina Marsiccobetre<sup>1</sup>, Ana M. Murillo<sup>1</sup>, Flávia S. Damasceno<sup>1</sup>, Richard B. M. M. Girard<sup>1</sup>, Leticia Marchese<sup>1</sup>, Luis A. Luévano-Martinez<sup>1</sup>, Renan W. Achjian<sup>1</sup>, Jurgen R. Haanstra<sup>2</sup>, Paul A. M. Michels<sup>3\*</sup>, Ariel M. Silber<sup>1\*</sup>

**1** Laboratory of Biochemistry of Tryps–LaBTryps, Department of Parasitology, Institute of Biomedical Sciences, University of São Paulo–São Paulo, Brazil, **2** Systems Biology Lab, Amsterdam Institute of Molecular and Life Sciences (AIMMS), Vrije Universiteit Amsterdam, Amsterdam, The Netherlands, **3** School of Biological Sciences, The University of Edinburgh, Edinburgh, United Kingdom

\* [paul.michels@ed.ac.uk](mailto:paul.michels@ed.ac.uk) (PAMM); [asilber@usp.br](mailto:asilber@usp.br) (AMS)



## OPEN ACCESS

**Citation:** Nascimento JF, Souza ROO, Alencar MB, Marsiccobetre S, Murillo AM, Damasceno FS, et al. (2023) How much (ATP) does it cost to build a trypanosome? A theoretical study on the quantity of ATP needed to maintain and duplicate a bloodstream-form *Trypanosoma brucei* cell. PLoS Pathog 19(7): e1011522. <https://doi.org/10.1371/journal.ppat.1011522>

**Editor:** Roberto Docampo, University of Georgia Athens, UNITED STATES

**Received:** March 23, 2023

**Accepted:** June 29, 2023

**Published:** July 27, 2023

**Copyright:** © 2023 Nascimento et al. This is an open access article distributed under the terms of the [Creative Commons Attribution License](https://creativecommons.org/licenses/by/4.0/), which permits unrestricted use, distribution, and reproduction in any medium, provided the original author and source are credited.

**Data Availability Statement:** All relevant data are within the manuscript and its [Supporting Information](#) files.

**Funding:** This work was supported by: Fundação de Amparo à Pesquisa do Estado de São Paulo (FAPESP) grants 2018/14432-3 and 2021/12938-0 (awarded to AMS), Conselho Nacional de Pesquisas Científicas e Tecnológicas (CNPq) grant 307487/2021-0 (awarded to AMS) and Wellcome

## Abstract

ATP hydrolysis is required for the synthesis, transport and polymerization of monomers for macromolecules as well as for the assembly of the latter into cellular structures. Other cellular processes not directly related to synthesis of biomass, such as maintenance of membrane potential and cellular shape, also require ATP. The unicellular flagellated parasite *Trypanosoma brucei* has a complex digenetic life cycle. The primary energy source for this parasite in its bloodstream form (BSF) is glucose, which is abundant in the host's bloodstream. Here, we made a detailed estimation of the energy budget during the BSF cell cycle. As glycolysis is the source of most produced ATP, we calculated that a single parasite produces  $6.0 \times 10^{11}$  molecules of ATP/cell cycle. Total biomass production (which involves biomass maintenance and duplication) accounts for ~63% of the total energy budget, while the total biomass duplication accounts for the remaining ~37% of the ATP consumption, with in both cases translation being the most expensive process. These values allowed us to estimate a theoretical  $Y_{ATP}$  of 10.1 (g biomass)/mole ATP and a theoretical  $Y_{ATP}^{max}$  of 28.6 (g biomass)/mole ATP. Flagellar motility, variant surface glycoprotein recycling, transport and maintenance of transmembrane potential account for less than 30% of the consumed ATP. Finally, there is still ~5.5% available in the budget that is being used for other cellular processes of as yet unknown cost. These data put a new perspective on the assumptions about the relative energetic weight of the processes a BSF trypanosome undergoes during its cell cycle.

Trust grant 222986/Z/21/Z (awarded to JFN and AMS). The funders had no role in study design, data collection and analysis, decision to publish, or preparation of the manuscript.

**Competing interests:** The authors have declared that no competing interests exist.

## Author summary

Cells use ATP as the main energy currency for the synthesis, organization and maintenance of their macromolecules and cellular structures, in order to stay alive and proliferate. For this purpose, ATP is produced from external nutrients, and is spent by cells in the many processes that are necessary for maintenance and building up new cells. Despite its relevance and the impressive quantity of biological data available, very little is known about how much ATP is required for maintaining and duplicating a cell. In this paper, we present a calculation on how much of the ATP produced by catabolism of the nutrient glucose is used to energize the different processes known to occur during the cell cycle of the infective form of the trypanosomatid parasite that causes human sleeping sickness, the bloodstream form of *Trypanosoma brucei*.

## Introduction

ATP hydrolysis provides most of the free energy used by cells to power biological processes including the metabolic reactions required to build up the biomass for cell proliferation and maintenance. It is possible to estimate the amount of ATP hydrolysis needed for most biological processes and thereby calculate the global ATP expenditure by a cell [1]. During the process of building a new cell, ATP hydrolysis is required for synthesis and polymerization of monomers such as dNTPs and rNTPs for nucleic acids, amino acids for proteins, fatty acids for phospholipids and monosaccharides for oligo- and polysaccharides. ATP hydrolysis is also required for the assembly of complex cell structures such as macromolecular complexes and organelles. Cells may acquire precursors for monomer synthesis or take up ready-to-use monomers from the extracellular environment, but these uptake processes also require ATP hydrolysis. Furthermore, ATP is necessary for other cellular processes that are not directly related to the synthesis of biomass, such as maintenance of membrane potentials and cellular shape, self-organization, motility, and turnover of molecules.

Parasitic organisms are intriguing in that they may differ in many aspects of their energy expenditure from their free-living counterparts. On the one hand, they may abandon (a sometimes very large) part of their biosynthetic activities if they can acquire multiple nutrients from their host. On the other hand, they may have to invest considerable energy in invasion of the host and in strategies to survive in an environment that tries to tame or kill them [2]. For the present work, we set out to estimate the energy expenditure of the trypanosomatid parasite *Trypanosoma brucei*. *T. brucei* is a unicellular flagellated parasite with a complex life cycle involving insect and mammalian hosts. During its life cycle, *T. brucei* transitions through different cell forms, each one adapted to the specificities of the environment it colonizes. In the gut of the insect vector—the tsetse fly—, amino acids such as proline are abundant and serve preferentially as the energy source for the so-called procyclic trypanosome when glucose is absent [3,4]. In the bloodstream of the mammalian host *T. brucei* can occur in two different developmental forms: long-slender, proliferating trypanosomes and short-stumpy forms. When triggered by a quorum-sensing mechanism, the long-slender trypanosomes differentiate to non-proliferating short-stumpy forms which are competent to develop into procyclic forms when ingested by a tsetse fly [5].

In the blood of the mammalian host, glucose is abundantly available, and it is well established that it is the main source of ATP used by the long-slender bloodstream form (BSF) of the parasite for its proliferation and to survive different environmental challenges [6,7]. Both procyclic and bloodstream forms of *T. brucei* can be easily cultivated *in vitro* in semi- or

completely defined media [8,9], which has enabled the detailed investigation of the end-products obtained from different substrates as well as the estimation of metabolic fluxes. In these organisms, the major part of the glycolytic pathway is compartmentalized in peroxisome-related organelles called glycosomes [10,11]. Noteworthy, while procyclic forms can oxidize metabolites (including glucose-derived pyruvate) in their single mitochondrion, under most conditions the BSF obtain their energy by aerobic fermentation with no involvement of oxidative phosphorylation (OxPhos).

The total energy cost of a biological process can be expressed as the summation of the direct costs (amount of the necessary ATP hydrolysis) spent on all energy-requiring processes [12]. In contrast to most bacteria and yeasts, BSF *T. brucei* use very little of the glucose consumed to synthesize biomass [12]. Noteworthy, these trypanosomes depend on extracellular availability of other essential nutrients to serve as carbon sources for the biosynthesis of precursors of macromolecules for biomass. Thus, the measured rate of glucose consumption, together with the fact that almost all glucose consumed by the BSF is directed to ATP formation allows calculation of the total amount of ATP produced per cell cycle. We can also estimate the ATP expenditure during a cell cycle as other relevant parameters are known such as doubling time, molecular content, genome size, transcriptome and proteome half-lives, and cell motility.

For some free-living prokaryotic and eukaryotic microorganisms, calculations of metabolic energy obtained (mostly transduced into ATP) from external sources have been reported previously ([13–15]. These calculations included energy obtained from external sources (oxidation of organic or inorganic molecules; absorbance of light) through different processes and the energy used for different activities (biosynthesis of macromolecules, biogenesis of (sub)cellular structures, transmembrane transport of molecules, motility, *etc.*). Here, we present a detailed estimation of the energy (ATP) budget and the energy costs of the two main commitments that a long-slender BSF *T. brucei* has during a cell cycle: to stay alive (maintenance) and to make a new cell (duplication). We found that the production of biomass, including the turnover of parts of its components under standard cultivation conditions, accounts for approximately 62% of the energy budget, with translation being the most “expensive” process. We estimated the extent to which several other cellular processes are responsible for using the remaining ATP that these cells produce.

## Results

### How much ATP is produced by *T. brucei* BSF during a cell cycle?

**The BSF *T. brucei* model studied.** The BSF of *T. brucei* is one of the relevant trypanosomatids for public health, and the availability of data about the various activities it exerts when parasitizing its mammalian hosts, such as proliferation, catabolic and anabolic processes, endocytosis, motility, among others led us to select it to estimate its ATP budget for cell maintenance during a cell cycle and for making an entirely new cell. Most data that we used for calculation of the ATP production have previously been obtained by using *T. brucei* strain Lister 427, BSF cell line 449 [13]. Trypanosomes of this Lister 427 strain are monomorphic, with the BSF occurring only as proliferating long-slender forms because they are incapable of differentiating to stumpy forms. Within specific cell population densities *in vitro* growth is exponential and the specific glycolytic flux is constant [12]. For the costs of making the building blocks of the cell such as dNTPs and amino acids, we used available data on the characterized biosynthetic pathways as well as the genome annotation for the presence of still uncharacterized pathways. For those biological processes in which energy costs are not yet fully understood for *T. brucei*, we made inferences based on data available for other organisms.

As previously mentioned, BSF *T. brucei* rely (almost) completely on glycolysis for their energy requirements and excrete nearly all pyruvate produced rather than further oxidizing it in the mitochondrion [12]. The first seven enzymes of the glycolytic pathway are compartmentalized in peroxisome-related organelles called glycosomes [11]. The reoxidation of the glycolytically produced NADH occurs through the transfer of the electrons by a shuttle mechanism from the glycosomes to the mitochondrion, in which glycolytically produced dihydroxyacetone phosphate is reduced to glycerol 3-phosphate with the concomitant oxidation of NADH to  $\text{NAD}^+$  by a glycosomal glycerol-3-phosphate dehydrogenase. In turn, the produced glycerol-3-phosphate is oxidized back to dihydroxyacetone phosphate by a mitochondrial glycerol-3-phosphate dehydrogenase, with the concomitant reduction of FAD to  $\text{FADH}_2$  which, in aerobic conditions, is reoxidized to FAD by the transfer of electrons to oxygen catalyzed by the trypanosome alternative oxidase [16]. Summarizing, this shuttle occurs without classical OxPhos [10,11]. In fact, in this stage of the parasite's life cycle, enzymes of the tricarboxylic acid (TCA) cycle are either absent or severely downregulated [17], and the  $\text{F}_1\text{F}_0$ -ATP synthase complex works in "reverse mode" accounting for an  $\text{H}^+$ /ATPase activity pumping protons into the intermembrane space, for the maintenance of the mitochondrial membrane potential [18–20]. Due to the absence of classical OxPhos, glycolysis is the main source of ATP in BSFs [21]. Net production of ATP, and thus the free-energy yield of glycolysis occurs in the cytosol and almost entirely comes from the flux through the enzyme pyruvate kinase [13]. It has been shown that some ATP synthesis can occur in the mitochondrion by the acetate:succinate CoA transferase / succinyl-CoA synthetase (ASCT/SCS) cycle, which can use as a substrate acetyl-CoA derived from relatively minute amounts of pyruvate routed to the mitochondrion and/or from threonine oxidation. However, the amount of ATP produced by this system is small when compared to that produced by glycolysis and may vary depending on conditions [10,22]. Taking all this information into account, we can proceed to make a reliable estimation of the total amount of ATP that is produced during a complete cell cycle, in which an entire *Trypanosoma* cell is built.

According to data from Haanstra et al. (2012) [13] when BSF *T. brucei* strain Lister 427, cell line 449 was growing exponentially in HMI-9 medium (for composition see S1 Table) at  $37^\circ\text{C}$  in the presence of 25 mM of glucose, the glucose consumption flux was  $160 \text{ nmol}/(\text{min} \times 10^8 \text{ cells})$ . It has been reported that 98% of consumed glucose ( $\sim 155 \text{ nmol}/\text{min} \times 10^8 \text{ cells}$ ) is directed towards pyruvate under aerobic conditions [23,24]. However, it should be noted that, depending on the culture conditions, a small part of glycolytically-derived metabolites can be used for the synthesis of sugar nucleotides [25], inositol [26], acetate [27,28], amino acids such as asparagine and alanine [28], which can contribute to anabolic processes. Stoichiometrically, the glycolytic breakdown of one molecule of glucose yields two molecules of pyruvate, and each of these is accompanied with the yield of one ATP, resulting in an ATP synthesis flux of  $310 \text{ nmol}/(\text{min} \times 10^8 \text{ cells})$ . This flux remains constant throughout the exponential proliferation phase [12], and therefore we calculated the total amount of ATP produced by one cell during one cell cycle (5.3 h in the experiment by Haanstra et al. 2012 [13]; for details see Materials and Methods), which results in  $6.0 \times 10^{11}$  molecules of ATP/(cell cycle  $\times$  cell). Considering that the total ATP concentration in mid-log cultured BSF *T. brucei* 427 is about 5 mM [29] and the cell volume  $45 \mu\text{m}^3$  [30], we estimated the number of moles of ATP/cell as being  $2.25 \times 10^{-16}$  moles, corresponding to  $1.3 \times 10^8$  ATP molecules/cell. As  $6.0 \times 10^{11}$  molecules of ATP are produced per cell cycle, the ATP pool is  $\sim 4,500$  times turned over during the cell cycle. With a cell cycle duration of 5.3 h (318 min), the ATP pool is turned over 14.5 times per minute.

**The cost of genome duplication.** To express and transmit its genetic information, every cell needs to duplicate and spatially organize its DNA, transcribe the information into RNA, and translate it into functional proteins. The energy requirements of each of these processes

differ and include the costs of making, assembling, and processing the building blocks of each polymer. Cells duplicate their genome once during the cell cycle, which requires activated nucleotides. It has been established for yeast and bacteria that the cost of *de novo* synthesis of all requisite nucleotides from glucose is approximately 50 ATPs per nucleotide [14]. Trypanosomatids lack the purine *de novo* biosynthetic pathway [31] and therefore rely on the purine salvage pathway by import of appropriate nitrogenous bases to be used as precursors for the synthesis [32]. In addition, trypanosomatids can synthesize pyrimidines from glutamine and aspartate, both present in the HMI-9 culture medium. So far, there is no evidence that it can import thymidine or thymine (reviewed in [33]). Based on the metabolic pathways predicted from the *T. brucei* genome for purine salvage and pyrimidines biosynthesis we calculated the ATP cost for the biosynthesis of each nucleotide (Table 1), starting from the precursors available in the culture medium: hypoxanthine (for purine salvage) and glutamine and aspartate (for the *de novo* synthesis of pyrimidines). The direct costs of making the other metabolites required in these pathways were also included (S2, S3 and S4 Tables). On average, *T. brucei* spends 11.5 ATP molecules for the biosynthesis of one purine and 9 ATPs for the biosynthesis of one pyrimidine (Table 1). The *T. brucei* haploid genome has an approximate size of 35 Mbp (TriTrypDB; <https://tritrypdb.org/tritrypdb/app>) and consists of 11 megabase chromosomes, a few intermediate chromosomes, and hundreds of minichromosomes [34]. Given the cost of each dNTP and the GC content of the *T. brucei* genome, the estimated total cost of the synthesis of the necessary number of dNTPs for the entire diploid genome duplication in one cell cycle is then  $1.4 \times 10^9$  ATPs.

Other costs involved in genome duplication were estimated. First, there is the cost of unwinding of the DNA double-helix. Using the yeast value, where this process costs one ATP per nucleotide [35], in *T. brucei* it will require  $7 \times 10^7$  ATPs in total. Next, some ATP is needed for the synthesis of the small RNA primers (~10 nt) necessary for the initiation of nucleotide polymerization during duplication of the lagging strand of DNA, which involves the formation of the Okasaki fragments. The number of the necessary RNA primers depends on the number of the origins of replication (ORI) and the size of the intervals between them. In yeast, the length of the Okasaki fragment is ~165 nt, with 10 nt corresponding to the RNA primer [36]. Taking into account that: i. the haploid genome has 35 Mb; ii. the lagging strand during DNA replication is fully replicated based on the synthesis of Okasaki fragments; and iii. that each Okasaki fragment has a length of ~165 nt, the total number of Okasaki fragments needed for the genome replication can be obtained from the ratio between the genome size and the length of the Okasaki fragment. The obtained value indicates that  $4.2 \times 10^5$  is the minimum number of RNA primers necessary to produce the Okasaki fragments necessary to duplicate the whole diploid genome. The average cost of rNTP synthesis in *T. brucei* is 5 ATPs per unit (see below). Therefore, the costs associated with RNA primer synthesis are  $2.1 \times 10^7$  ATPs. After the synthesis of Okasaki fragments, DNA ligase uses 2 ATPs to ligate each pair of fragments, which then costs  $8.4 \times 10^5$  ATPs in this parasite. Last, there is an ATP cost associated with the assembly of the polymerase-containing sliding clamp. On average, 3 ATPs per complex are

**Table 1. ATP cost for the synthesis of deoxyribonucleotides for *T. brucei* genome duplication.**

dNTP	ATP cost	% of the genome	Total cost
dCTP	12	22.8	$3.8 \times 10^8$
dTTP	6	27.2	$2.3 \times 10^8$
dATP	11	27.2	$4.2 \times 10^8$
dGTP	12	22.8	$3.8 \times 10^8$
<b>Total</b>			<b><math>1.4 \times 10^9</math></b>

<https://doi.org/10.1371/journal.ppat.1011522.t001>

**Table 2. Summary of ATP costs associated with nuclear and mitochondrial genome duplication (maxicircles and minicircles) of *T. brucei*.**

Process	ATP cost		
	Nuclear genome	Maxicircles	Minicircles
dNTP synthesis	1,400 x 10 <sup>6</sup>	6.9 x 10 <sup>6</sup>	60 x 10 <sup>6</sup>
DNA unwinding	70 x 10 <sup>6</sup>	0.69 x 10 <sup>6</sup>	6 x 10 <sup>6</sup>
RNA primer synthesis	21 x 10 <sup>6</sup>	0.21 x 10 <sup>6</sup>	1.8 x 10 <sup>6</sup>
Okasaki fragments ligation	0.84 x 10 <sup>6</sup>	0.0084 x 10 <sup>6</sup>	0.073 x 10 <sup>6</sup>
Sliding clamp assembly	1.3 x 10 <sup>6</sup>	0.012 x 10 <sup>6</sup>	0.11 x 10 <sup>6</sup>
Opening of ORIs	negligible	negligible	0.12 x 10 <sup>6</sup>
Total	<b>1,493 x 10<sup>6</sup></b>	<b>7.8 x 10<sup>6</sup></b>	<b>68.1 x 10<sup>6</sup></b>

<https://doi.org/10.1371/journal.ppat.1011522.t002>

necessary [37]. Since duplication of the lagging strand requires one sliding clamp per fragment to be synthesized, *T. brucei* requires approximately 1.3 x 10<sup>6</sup> ATPs in this step. As a whole, the contribution of these processes to the total cost is minor when compared to the cost of nucleotide synthesis (Table 2).

There is still a series of costs that is too small to be relevant to the total cost of genome duplication. One example is the ATP investment associated with opening the ORIs. It has been estimated as being at least 20 ATPs per ORI [14]. In *T. brucei*, there is a minimum number of 33 ORIs necessary to replicate the 11 megabase chromosomes [38], which adds at least 1,320 ATP molecules per S-phase of the cell cycle. Additionally, *T. brucei* has at least 6 intermediate-sized chromosomes and about 50–100 minichromosomes [39]. Assuming that there is at least one ORI per intermediate and minichromosome, there will be an additional requirement of about 620 to 2,120 ATP molecules. Other costs such as for proofreading, DNA repair, and epigenetic modifications are still to be fully elucidated. The total cost for the nuclear genome duplication is estimated as being 1.49 x 10<sup>9</sup> ATP molecules.

### The cost of kDNA duplication

The mitochondrial genome of *T. brucei* is contained in a unique structure called the kinetoplast. The DNA present in the kinetoplast (kDNA) consists of a concatenated network of two classes of circular DNA: the maxicircles (~23 kb) and minicircles (~1 kb). Maxicircles are present in a low-copy number (~30 per cell) and encode proteins of the mitoribosomes, some of the proteins of the complexes of the respiratory chain, and two rRNAs. Remarkably, most of these genes in maxicircles are encrypted and their transcripts need to undergo editing before translation. The RNA editing process is mediated by guide RNAs (gRNAs) that are transcribed from the minicircles. There are approximately 6,000 minicircles per cell with at least 391 different sequences encoding different gRNAs [40]. Because of the intricate nature of the kDNA, the process of its duplication is rather complex. On one hand, minicircles are released from the core of the network, unwound, duplicated and then reassembled back in the periphery of the network. On the other hand, maxicircles are duplicated inside the network, but the exact mechanism is still unknown (reviewed in [41]).

As has been described for genome replication, dozens of proteins participate in kDNA duplication, including helicases, topoisomerases, polymerases, primases and ligases (reviewed in [42]). As the same classes of proteins are involved in both processes, we assumed similar costs for the initiation of each replication unit to those estimated for the nuclear genome duplication. Therefore, we used the rationale and estimations described in the previous section: (i) DNA unwinding, which costs 1 ATP per nucleotide, resulting in 0.69 x 10<sup>6</sup> ATPs for maxi- and 6 x 10<sup>6</sup> ATPs for minicircle duplication; (ii) RNA primer synthesis costs 50 ATPs per

primer, resulting in  $0.21 \times 10^6$  ATPs for maxi- and  $1.8 \times 10^6$  ATPs for minicircles; (iii) Okasaki fragments ligation costs 2 ATP per ligation resulting in  $0.0084 \times 10^6$  ATPs for maxi- and  $0.073 \times 10^6$  ATPs for minicircles; and (iv) sliding clamp assembly which costs 3 ATPs on average, resulting in  $0.012 \times 10^6$  ATPs for maxi- and  $0.11 \times 10^6$  ATPs for minicircles (Table 2).

Some peculiarities regarding the kDNA and its replication required an adjustment in the calculations. First, although the sequence of kDNA is mostly known, the distribution of the 391 types of minicircles varies from 1 to 144 copies per cell [40]. This makes the accurate GC-content hard to estimate. For this reason, we assumed a 50% CG content and an average synthesis cost of 10 ATPs per nucleotide. Accordingly, the cost of the dNTPs for maxicircle duplication is  $6.9 \times 10^6$  ATPs and  $60 \times 10^6$  ATPs for minicircle duplication. Second, according to the calculations made for nuclear genome DNA replication, the cost for opening the origins of replication is 20 ATPs per ORI. We have previously considered this cost negligible due to the low number of ORIs necessary to duplicate the whole nuclear genome. Although this number is still negligible for the duplication of maxicircles (~600 ATPs), due to the number of minicircles (20 ATPs per ORI for 6,000 ORIs), this cost becomes more relevant for their duplication, and it totalizes  $0.12 \times 10^6$  ATP molecules (Table 2). The duplication of the mitochondrial genome (maxicircles and minicircles) costs  $0.0759 \times 10^9$  ATP molecules. In total, duplicating both the nuclear and the mitochondrial genome requires an estimated  $1.57 \times 10^9$  ATP molecules.

### The cost of transcription of the nuclear genome

In *T. brucei* BSF, RNA Pol I transcribes the gene arrays for ribosomal RNAs (rRNAs) and a telomeric expression site containing a single variant surface glycoprotein (VSGs) gene. This specific gene comes out of a very large repertoire of which one VSG is expressed at a given time. However, together with this VSG gene, a set of genes called Expression Site Associated Genes (ESAGs) are transcribed that lie upstream of the VSG gene [43–45]. Most of them encode proteins with still unknown biological function. RNA Pol II transcribes all other protein-coding genes as well as the genes for a spliced leader (SL) RNA, whilst RNA Pol III transcribes genes encoding snRNAs, tRNAs, and 5S RNAs [46,47]. In trypanosomatids, genes are organized in tandem arrays which are transcribed in a polycistronic manner. The resulting long precursor RNAs are processed by *trans*-splicing and polyadenylation. Consequently, mature individual mRNAs containing a 39 nt SL with a 5' cap and a 3' poly-A tail are produced [48]. It means that, differently from organisms that regulate transcription initiation and termination of each gene, trypanosomatids transcribe coding genes that are not needed in a specific condition (e.g. the tandemly-arranged genes encoding PGKA, B and C are all transcribed simultaneously, but B or C is degraded depending on the life-cycle stage [49–51]), as well as intergenic regions and then degrade them once the mature mRNAs are formed.

Regarding the ATP costs of transcription, we estimated the ATP costs for synthesis of an entire set of transcripts and the ATP costs associated with their maintenance (turnover). For that purpose, we used most of the data and assumptions used for the model developed by Haanstra and collaborators for different aspects of BSF *T. brucei* gene expression [51]. In this paper, they also reported values and estimations for numbers and half-lives of four types of RNAs: i. rRNAs; ii. RNAs encoding VSGs; iii. mRNAs; iv. SL-RNAs (Table 3). For the ATP expenditure calculation, we considered the cost of synthesis of the rNTPs to be used as monomers, the cost of each polymerization reaction, and the steady-state number of molecules of each RNA-type produced per cell ( $N$ ) and the average length of the mature RNA ( $L$ ).

**Synthesis of the transcriptome.** The production cost of the nucleotides is on average 5 ATPs per rNTP (Tables 4 and S3). The total synthesis cost for the four RNA populations is 5 x



Table 3. Data from Haanstra et al., 2008 [52] used in this work.

Process	rRNA	VSG mRNA	Total other mRNAs	SL-RNA
Number of molecules per cell (N)	125,000	1,000	19,000	20,000
Half-life	12 h	45 min	30 min	30 min
Transcript length*	8,550 nt	1,720 nt	2,800 nt	141 nt
Mature transcript length (L)	6,100 nt	1,720 nt	2,200 nt	39 nt

\*The value for the transcript VSG 117 was mistyped in Haanstra et al. (2008) and is corrected here on the basis of [52]

<https://doi.org/10.1371/journal.ppat.1011522.t003>

$N \times L$  [15]. Therefore, the resulting synthesis cost for the rRNA population is  $5 \times 125,000 \times 6,100 = 380 \times 10^7$  ATPs, for the VSG mRNAs  $0.86 \times 10^7$  ATPs, for the set of other mRNAs  $21 \times 10^7$  ATPs and for the SL-RNAs  $0.35 \times 10^7$  ATPs per cell cycle (Table 5).

**Maintenance of the transcriptome (turnover).** Assuming that ribonucleotides are efficiently recycled, the cost invested in recharging the rRMPs to rRTPs is 2 ATPs [14]. Considering the half-lives ( $t_{1/2}$ ) of each set of RNAs, the maintenance cost is the cost of replacing the RNAs degraded during the cell cycle. Given the doubling time of BSF *T. brucei*, here taken as 5.3 hours (see above) and the half-life of each set of RNA, we calculated the number of RNA molecules of each class that must be resynthesized during a cell cycle for replacement ( $N_r = 1 - N(t)$ ) where  $N(t)$  is calculated by using the exponential decay function:

$$N(t) = N_0 \times \left(\frac{1}{2}\right)^{\frac{t}{t_{1/2}}}$$

in which  $N(t)$  is the remaining number of molecules after a given time  $t$ ,  $N_0$  is the initial number of molecules,  $t_{1/2}$  is the average half-life of each set of RNA molecules, and  $t$  is the time considered (here the time for the completion of a cell cycle). We obtained that  $N_r$  is 32,965 for rRNAs, 993 for VSG mRNAs, 18,988 for all other mRNAs and 19,987 for the SLs. Hence, as we considered a complete recycling of the ribonucleotides obtained from the RNA degradation (NMPs), the cost for maintaining the whole transcriptome is the cost of recharging the nucleotides to be polymerized. For each RNA subset we calculated the cost as  $2 \times N_r \times L$ . According to this, the total cost for the maintenance of each type of RNA is  $40 \times 10^7$  for rRNAs and  $0.34 \times 10^7$  ATPs for VSG mRNAs, whereas the maintenance of the remaining set of mRNAs costs  $8.3 \times 10^7$  ATPs, and the cost calculated for SL-RNAs is  $0.14 \times 10^7$  ATPs (Table 5).

**Polymerization of rNTPs of intergenic regions.** As the intergenic regions are transcribed and degraded to monomers after RNA processing, we considered that the ribonucleotides used in the transcription of intergenic regions are efficiently recycled. However, the cost invested in polymerizing the ribonucleotides of the intergenic regions must be estimated. For this purpose, we used the difference in length between the whole precursor and the mature transcripts and applied the same calculations for the polymerization costs of the intergenic regions as used for those to calculate the cost of the synthesis and maintenance of the mature transcriptome [52]. For the VSG transcripts, the whole transcript length is considered as being

Table 4. ATP cost for the synthesis of ribonucleotides.

rNTP	ATP cost
CTP	5
UTP	4
ATP	5
GTP	6

<https://doi.org/10.1371/journal.ppat.1011522.t004>

Table 5. Summary of costs in molecules of ATP associated with nuclear transcription per cell cycle of *T. brucei*.

Process	Synthesis	Maintenance	Total ATP cost
rRNA	380 x 10 <sup>7</sup>	40 x 10 <sup>7</sup>	420 x 10 <sup>7</sup>
VSG mRNA	0.86 x 10 <sup>7</sup>	0.34 x 10 <sup>7</sup>	1.2 x 10 <sup>7</sup>
other mRNA	21 x 10 <sup>7</sup>	8.3 x 10 <sup>7</sup>	29.3 x 10 <sup>7</sup>
SL RNA	0.35 x 10 <sup>7</sup>	0.14 x 10 <sup>7</sup>	0.49 x 10 <sup>7</sup>
nucleosome displacement*	0.12 x 10 <sup>7</sup>	-	0.12 x 10 <sup>7</sup>
polymerization intergenic regions	169.75 x 10 <sup>7</sup>	23.72x10 <sup>7</sup>	193.47 x 10 <sup>7</sup>
<i>trans</i> -splicing	0.02 x 10 <sup>7</sup>	0.019 x 10 <sup>7</sup>	0.039 x 10 <sup>7</sup>
<b>Total</b>	<b>572.1 x 10<sup>7</sup></b>	<b>72.52 x 10<sup>7</sup></b>	<b>644.62 x 10<sup>7</sup></b>

\* This is an estimation of the minimum ATP cost for this process. Due to the lack of experimental data, it is not possible to determine the contribution of this cost to the maintenance of the RNA pools.

<https://doi.org/10.1371/journal.ppat.1011522.t005>

the same of the mature transcript length [51,52]. However, VSG genes are transcribed together with the ESAGs in a polycistronic manner in one out of the about 15 telomeric bloodstream expression sites (BES) that is activated. Therefore, we calculated the total length of the intergenic regions of the polycistron. For this, we used data from the BES 40 containing the VSG 221 gene [53]. The whole length of BES 40 is 59.78 kb. It contains 18 protein-coding sequences including the VSG with a cumulative length of 25.15 kb. For the estimation of the UTR regions (which are also part of the mature RNAs) we used the median length of 130 nt for the 5' UTR and 399 nt for the 3' UTR [54] except for the VSG, where we considered the whole size of 1,720 nt [51,52]. So, the total length of the polycistron that is maintained as mRNA is 34.44 kb. Therefore, the intergenic regions that are transcribed and further degraded are estimated as being 25.34 kb long. Applying the same calculations for synthesis ( $5 \times N \times L$ ) and maintenance ( $2 \times Nr \times L$ ) for the polymerization used above, we estimated the total cost of intergenic transcription for synthesis of a new set of rRNAs, VSG/ESAGs, mRNAs of other proteins, and SL-RNAs as being  $150 \times 10^7$ ,  $13 \times 10^7$ ,  $5.7 \times 10^7$  and  $1.05 \times 10^7$  ATPs, respectively, per cell cycle. Additionally, the cost for polymerizing intergenic regions during the maintenance of the RNA pools is  $16 \times 10^7$  for rRNAs,  $5 \times 10^7$  for VSGs/ESAGs,  $2.3 \times 10^7$  for mRNAs of other proteins, and  $0.42 \times 10^7$  for SL-RNAs (Table 5).

**Nucleosome displacement.** Another cost associated with transcription is related to the displacement of the nucleosomes. This process involves various histone posttranslational modifications [55]. *T. brucei* expresses four out of the five canonical eukaryotic variants of histones (H2A, H2B, H3, and H4) and they serve as boundaries for polycistronic units [56,57]. The length of DNA wrapped around each nucleosome is ~147 nt and the length of the strands linking two nucleosomes is ~43 nt in *T. brucei* [58]. Considering these numbers and the total DNA length, the number of nucleosomes can be estimated as being  $3.7 \times 10^5$  per diploid genome. Assuming a minimum cost of 30 ATPs per set of modifications in one nucleosome [14] and that once the chromatin is open for transcription it remains in this state, the minimum cost of displacing the nucleosome barriers during transcription is  $1.1 \times 10^6$  ATPs per cell cycle (Table 5).

**Splicing.** By far the major part of the mRNA maturing process occurs by *trans*-splicing (with only two exceptions reported [59]). In *trans*-splicing, similarly to *cis*-splicing, two transesterification reactions unite two RNA fragments (reviewed in [54]). *Cis*-splicing costs at least 10 ATPs per intron [14,60] and here we consider the same cost for *trans*-splicing. Considering the synthesis and maintenance of mRNA levels, the cost of *trans*-splicing in a new set of mRNAs is  $10 \times N$ , which results in  $2 \times 10^5$  ATPs per cell cycle. Additionally, the cost of *trans*-

splicing during the maintenance of mRNA levels is  $10 \times N_r$ , resulting in  $1.89 \times 10^5$  ATPs per cell cycle (Table 5).

In summary, transcription of the nuclear genome costs  $\sim 6.4 \times 10^9$  ATP molecules. Costs associated with other aspects of transcription such as the formation of the transcriptional complexes are too small or have not been completely elucidated and therefore are not considered here. As an example, in eukaryotes, RNA pol II transcription initiates with the recruitment of the polymerase to the promoter region by multiple transcription factors. Subsequently, the DNA helix is unwound, forming an open complex (OC). These processes cost at least 20 ATPs per OC [14,61,62]. Because of the polycistronic transcription, fewer OCs are necessary to initiate transcription in trypanosomatids. As there are no available data for the cost of the formation of OCs for RNA polymerases I and III, we estimated the cost of the OCs for the genes transcribed by RNA pol II. In the 11 pairs of megabase-size chromosomes there are  $\sim 380$  RNA pol II transcribed polycistronic units in the housekeeping regions [63] with an estimate of 50 genes per polycistron. If we consider that once the OC is formed it remains open during all rounds of transcription, 380 OCs are needed to initiate transcription by RNA pol II. This results in a minimum cost for OCs of  $\sim 7.6 \times 10^3$  ATPs per cell cycle. On the other hand, we can consider that one OC is formed on each round of transcription. In that case, the necessary OCs for RNA II pol transcription can be estimated as:

$$\text{OC} = (N + N_r)/50 = 760$$

Thus,  $\sim 760$  OCs are necessary for RNA pol II transcription, resulting in a cost of  $1.5 \times 10^4$  ATPs per cell cycle. Either way, these costs are negligible to the total transcriptional cost. Similarly, transcriptional termination is likely to be less costly in trypanosomatids, since it happens at transcription termination sites marked by histone variant H3.V and base J, a modified thymine detected in the nuclear DNA of trypanosomatids and related protists grouped in the Euglenozoa clade [64,65]. Additionally, some transcriptional costs have not been completely elucidated. For example, phosphorylation of the C-terminal domain of RNA pol II regulates different aspects of transcription [66]. However, the number of phosphorylation events per transcriptional cycle in trypanosomatids has not been determined yet. Another process related to transcription of which the exact costs are difficult to calculate is RNA nuclear export. Interestingly, although this process is ATP dependent in opisthokonts [67], the lack of many ATPases in the nuclear pore complex of trypanosomatids suggests that mRNA nuclear export is GTP driven in these organisms [68,69]. Assuming that the amount of HEBs (high-energy bonds) consumed by *T. brucei* for RNA nuclear export is the same as that consumed by yeast (*i.e.*, 2 ATP molecules per transcript) [70,71] we can estimate a cost for the export of the total number of rRNAs (those for maintenance and those for duplication) minus the SL-RNAs, which remain in the nucleus. The total HEB equivalent to ATP used for this process is  $3.1 \times 10^5$  for rRNAs,  $4.0 \times 10^3$  for VSG mRNAs and  $7.6 \times 10^4$  for all other mRNAs. Therefore, under the assumption that the cost per RNA exported from the trypanosome nucleus to the cytoplasm is similar to that in yeast, the total cost for RNA export is  $3.9 \times 10^5$  HEBs, equivalent to ATP molecules. Regardless of the case, these costs remain to be determined with more precision.

### The costs of transcription of kDNA

The maxicircles of the kDNA code for 2 rRNAs and 18 proteins [72]. It is currently accepted that, similarly to what happens in the trypanosomatid nucleus and mitochondria of other organisms, transcription of the maxicircles is polycistronic and that the long pre-RNAs are processed at both ends to generate mature RNAs [73,74]. However, it has been recently

proposed that this transcription might be gene-specific and promoter-regulated [75,76]. Additionally, transcripts from 12 of these genes, named cryptogenes, need to undergo further processing by RNA editing to generate translation-competent mRNAs. This editing consists of the insertion and/or deletion of uridines and is mediated by gRNAs transcribed from the minicircles present in the kDNA (reviewed in [77]). Once transcribed, these gRNAs are also processed by 3'-5' trimming and U-tailing and stabilized by their ligation to the RNA-editing substrate-binding complex (RESC) (reviewed in [76]). Multiple gRNAs are necessary for the editing of a single maxicircle-encoded mRNA ([78]).

To estimate the minimal cost of kDNA transcription, and due to the lack of data on the number of kDNA transcripts per BSF cell and their half-lives, we assumed that maxicircle transcription has similar dynamics to that of nuclear transcription. Noteworthy, expression of most of the mtDNA genes is developmentally regulated but, in the model of polycistronic transcription, this regulation is likely to be posttranscriptional [74]. Thus, considering a similar ratio of the number of transcripts/genes to the nucleus, and the number of maxicircles (~30) present in the kDNA, we estimated an average of 480 molecules of mRNA and 35,700 molecules of rRNA per BSF mitochondrion. The average length of the mature fully-edited mitochondrial rRNAs and mRNAs was considered to be 880 nt and 933 nt, respectively [72]. With a cost of 5 ATPs for the synthesis of each rNTP (Table 4), efficient recycling of the ribonucleotides once the RNAs are degraded, 2 ATPs for recharging each monomer [14], and similar half-lives to those RNAs encoded by the nuclear genome, we calculated that  $17.3 \times 10^7$  and  $0.3 \times 10^7$  ATP molecules are necessary to synthesize the estimated pool of mitochondrial rRNAs and mRNAs, respectively. In the polycistronic model of transcription, intergenic regions are transcribed and, after RNA processing, the rNTPs are recycled. For that reason, it is necessary to estimate the polymerization cost of the intergenic regions of the polycistrons transcribed from the maxicircles. Given the size of each maxicircle (~23 kb) and the sum of the average length of mature RNAs (18,554 nt) we considered that 4,446 nt are polymerized for each maxicircle, resulting in a consumption of  $\sim 2.7 \times 10^5$  ATP molecules.

To have a more complete estimation of the total transcriptional cost of the mitochondrial genome, it is necessary to estimate the cost of the transcription of gRNAs. Transcription of the minicircles generates an 800 nt precursor [79], encoding 2–5 gRNAs each, with an average length of 49 nt [80]. It means that, on average, for each minicircle, 678 rNTPs are polymerized and then recycled after processing. Considering the number of 6,000 minicircles per cell [40] and that at least one of each gRNA will be transcribed, the minimal cost for minicircles transcription is the cost of the polymerization of the rNTPs of the intergenic regions, which is  $\sim 0.8 \times 10^7$  ATP molecules, plus the cost of synthesis and polymerization of the rNTPs in the mature gRNAs, which is  $\sim 0.4 \times 10^7$  ATP molecules. Thus, transcription of the minicircles costs, at minimum,  $1.2 \times 10^7$  ATPs per cell cycle.

Assuming that transcription of maxicircles has a similar global dynamic as that of nuclear transcription, and that each minicircle is only transcribed once per life cycle, we calculated the cost of transcription of the mitochondrial genome at  $18.8 \times 10^7$  ATP molecules (Table 6). It is worth mentioning that these are likely underestimations due to the scarce knowledge of the ATP expenditure of each process involved in kDNA transcription, pre-RNA processing and

**Table 6. Summary of ATP costs per cell cycle associated with kDNA transcription.**

Process	Maxicircles	Minicircles
Transcription	$17.6 \times 10^7$	$0.4 \times 10^7$
Polymerization of intergenic regions	$0.03 \times 10^7$	$0.8 \times 10^7$
<b>Total</b>	<b><math>17.6 \times 10^7</math></b>	<b><math>1.2 \times 10^7</math></b>

<https://doi.org/10.1371/journal.ppat.1011522.t006>

mRNA editing. However, it should be noted that even if kDNA transcription would be several folds more expensive, it remains small in relation to the total cellular transcription cost.

### Energy expenditure for proteome synthesis, maintenance, degradation

Regarding the biosynthesis of proteins, we must take into account the cost of obtaining their components, the amino acids. For this, we consider two sources for these metabolites: their uptake from the environment, and their biosynthesis *de novo*. The present work is based on data obtained by culturing the parasites in a very rich medium containing all the amino acids, so in this condition, and probably also *in vivo* in the bloodstream, it is reasonable to assume that most of their requirements are fulfilled through their acquisition from the extracellular medium. However, we made also an estimation of the cost of the *de novo* synthesis for those amino acids having their biosynthetic pathways predicted from the genome sequence as this estimation could be of general interest (see [S1 Text](#)).

To determine how much ATP is spent by BSF *T. brucei* on protein synthesis, we first estimated the number of amino acids present in its proteome from the cell's known volume and the calculated protein density. The volume of *T. brucei* BSF (1K1N, *i.e.* one kDNA network and one nucleus, after cell division, before DNA replication) cells is  $\sim 45 \mu\text{m}^3$  [30]. According to the method proposed by Milo (2013) [81], we calculated the number of proteins per cell based on the protein mass per unit volume ( $c_p$ ) in grams of protein per milliliter of cell volume, which has been estimated for several cell types as being 0.2 g/ml [81,82]. Other relevant parameters taken into account are the average length of proteins ( $l_{aa}$ ) (300 amino acids according to [83]), and the average molecular mass of amino acids ( $m_{aa}$ ) (110 Da). Therefore,  $l_{aa} \times m_{aa}$  is the average molecular mass per protein and the molar concentration of proteins is:

$$\frac{N}{V} = \frac{c_p}{l_{aa} \times m_{aa}} = 6.1 \text{ mM}$$

where  $N/V$  is the average number of moles of proteins per unit volume. For converting these values into the number of proteins per  $\mu\text{m}^3$ , we applied the following equation:

$$\frac{N}{V} = 6.1 \times 10^{-3} \text{ Molar} \times N_A \times 10^{-12} \frac{\text{ml}}{\mu\text{m}^3}$$

where  $N_A$  is Avogadro's number. The obtained value is  $3.7 \times 10^6$  proteins/ $\mu\text{m}^3$ . Therefore, considering a cell volume of  $45 \mu\text{m}^3$  we obtained a number of proteins per cell of  $166.5 \times 10^6$ .

With an average protein length of 300 amino acids [83], we then calculated that a single cell contains  $5.0 \times 10^{10}$  amino acids as protein components (in other words, forming peptide bonds). The direct cost of polymerization is 4 ATPs per amino acid [84], so the direct cost of translation, for a single cell, is about  $\sim 2.0 \times 10^{11}$  ATPs to double the entire set of proteins (Table 7).

During the BSF trypanosome's cell cycle, part of its proteins has to be degraded and replaced by new proteins to be synthesized. The balance between these processes represents

**Table 7. Summary of ATP costs associated with protein synthesis and degradation during a cell cycle of BSF *T. brucei*.**

Process	ATP cost
Proteome doubling	$1.9 \times 10^{11}$
Protein degradation	$0.18 \times 10^{11}$
Protein resynthesis	$1.4 \times 10^{11}$
<b>Total</b>	<b><math>3.48 \times 10^{11}</math></b>

<https://doi.org/10.1371/journal.ppat.1011522.t007>

the cell's protein turnover. Its cost must be added to that of the entire proteome doubling during the parasite's growth and division. We considered for our calculations only regulated protein degradation, which requires an expenditure of 100–200 ATP molecules per degraded protein [14,85]. Here we assumed an average value of 150 ATPs per degraded protein. A proteomic turnover study determined that this process is directly influenced by the duration of the cell cycle. For this, the duration of BSF trypanosomes cell cycle was determined as being 11.85 h. This remarkable difference with the duration considered in our study can be explained by the fact that the authors performed this estimation for parasites growing under protein labeling conditions (data were obtained using SILAC labeling for proteomics). Under these conditions, the estimated a half-life for the entire proteome was 5.6 h [86]. As we are using, in this work, the duration of the BSF cell cycle of 5.3 h, we made an estimation of energy cost of the proteome's turnover in our model by scaling the half-life using the rationale described in Tinti et al. (2019) [86]. The obtained value for the proteome half-life was then 2.56 h, meaning that, according to the exponential decay law, during an entire cell cycle 76% of the proteome is degraded. Therefore,  $1.2 \times 10^8$  proteins per cell are degraded during a cell cycle, at a total cost of  $1.8 \times 10^{10}$  ATP molecules (Table 7). At the same time, to maintain the entire proteome, the same quantity of these proteins must be newly synthesized at a cost of  $1.4 \times 10^{11}$  ATP (Table 7). This, added to the synthesis of an extra net set of proteins for obtaining an entire proteome for each daughter cell, requires  $3.3 \times 10^{11}$  ATP molecules per cell cycle for protein synthesis. In summary, the total cost for degradation, resynthesizing and doubling of the proteome is  $\sim 3.5 \times 10^{11}$  ATP molecules (Table 7).

### Energy cost of sugar nucleotides used in the synthesis of the VSG coat

In the BSF of *T. brucei*, the major surface protein is the VSG, which is highly glycosylated. The VSG polypeptide is estimated as being present in  $10^7$  copies per cell, representing approximately 90% of cell surface polypeptides and 10% of total cellular protein content [87]. Therefore, the sugar nucleotides used in the synthesis of the VSGs require by far the major part of the ATP dedicated to the synthesis of the entire pool of sugar nucleotides in these cells. Trypanosomatids' survival, infectivity, and virulence in their mammalian hosts are directly influenced by their cell surface glycoconjugates. The amount of sugar nucleotide used for their synthesis was calculated based on previous estimates [25]. For this, certain conditions were assumed: i) the metabolites are evenly distributed throughout the cell volume; ii) the demand for each sugar nucleotide is minimal and for this calculation we did take into account the glycoconjugates turnover; iii) the contributions of low-abundance glycoconjugates are considered negligible; and iv) an average glucidic composition of  $\text{Man}_{15}\text{GlcNAc}/\text{GlcN}_{5,5}\text{Galp}_5$  [87], based on that of VSG variant 221 (a.k.a. MITat 1.2). On these bases, we estimated the need for  $5 \times 10^7$  UDP-Galp, and the same quantity of UDP-GlcNAc. Also,  $15 \times 10^7$  units of GDP-Man are required. Considering an average ATP expenditure of 4 HEBs per nucleotide sugar, the total ATP requirement for synthesizing the glucidic moieties of  $10^7$  VSGs is  $\sim 1 \times 10^9$  ATP molecules per cell during a cell cycle (Table 8).

**Table 8. Estimation of ATP cost for the synthesis of sugar nucleotides for *T. brucei* VSGs per cell cycle.**

Sugar Nucleotide	HEBs per molecule	SN in VSG	HEBs per SN	HEBs per cell
UDP-Galp	4	5	20	$2 \times 10^8$
UDP-GlcNAc	4	5	20	$2 \times 10^8$
GDP-Man	4	15	60	$6 \times 10^8$
			<b>Total</b>	<b><math>1 \times 10^9</math></b>

<https://doi.org/10.1371/journal.ppat.1011522.t008>

Table 9. Lipid composition and energy cost of biosynthesis for each molecular species in BSF of *T. brucei*.

Species	%mol	[Conc.] (nmol per mg protein)	Number of HEBs for biosynthesis	nmol <sub>HEB</sub> per ug protein	nmol <sub>HEB</sub> per parasite	ATP molecules per parasite
PC	47.8	171.6	4	686.4	$6.86 \times 10^{-6}$	$4.1 \times 10^9$
PE	20.7	74.313	4	297.252	$2.97 \times 10^{-6}$	$1.8 \times 10^9$
PI	5.4	19.386	4	77.544	$7.75 \times 10^{-7}$	$4.7 \times 10^8$
PS	3	10.77	4	43.08	$4.31 \times 10^{-7}$	$2.6 \times 10^8$
CL <sup>1</sup>	0.715	2.56	8	20.48	$2.05 \times 10^{-7}$	$1.2 \times 10^8$
PG <sup>1</sup>	0.485	1.74	4	6.96	$6.96 \times 10^{-8}$	$4.2 \times 10^7$
Ergosterol <sup>2</sup>	13.8	49.54	12	594.48	$5.94 \times 10^{-6}$	$3.6 \times 10^9$
SM	14.5	52.055	4 (5 for IPC or EPC)	247.7	$2.48 \times 10^{-6}$	$1.5 \times 10^9$
<b>Total</b>					<b><math>1.97 \times 10^{-5}</math></b>	<b><math>1.19 \times 10^{10}</math></b>

PC, phosphatidylcholine; PE, phosphatidylethanolamine; PI, phosphatidylinositol; PS, phosphatidylserine; CL, cardiolipin; PG, phosphatidylglycerol SM, sphingomyelin. <sup>1</sup> Based on the molar fraction of PG/CL found in the procyclic form; <sup>2</sup> compositions were observed in neutral fractions. E.U., Elementary Units.

<https://doi.org/10.1371/journal.ppat.1011522.t009>

### Energy expenditure for doubling the lipidome of *T. brucei* BSF

One of the basic needs for cell proliferation is the production of a new set of lipids for synthesizing the external and internal membranes. However, we have not found in the literature an estimate of the total energy cost necessary for doubling the total cell membrane content. BSF *T. brucei* can obtain its lipids by two different routes [88,89]: either from the mammalian host plasma, mainly by receptor-mediated endocytosis of LDL particles [90] or by *de novo* synthesis. The contribution of both routes may vary dependent on external conditions. A calculation of the cost of lipid acquisition by uptake from the host is an integral part of the estimation of the total cost of the formation of endocytic vesicles described below. Given that *T. brucei*'s total pool of phospholipids and sterols [91–93], as well as their biosynthesis pathways [94–97] have been characterized in detail, it allowed us to estimate the energy requirements when doubling of the lipidome content of BSF trypanosomes would entirely occur by *de novo* routes. For this purpose, we considered the number of HEBs used in the biosynthetic pathways of each species of phospholipid and ergosterol. With this information, we were able to estimate the amount of ATP needed for their doubling (Table 9).

The total amount of ATP consumed during the cell cycle of *T. brucei*, for the entire lipidome doubling (which includes the cost of membrane doubling) is  $1.19 \times 10^{10}$  ATP molecules. Noteworthy, among the costs calculated (Table 9), the lipid species that are most energy demanding are ergosterol (36%), PC (31.6%), PE (13.7%) and SM (12%), respectively.

### Energy expenditure on polyphosphate synthesis

Polyphosphates (polyP) are linear polymers of a few to many hundreds of inorganic phosphate (Pi) residues linked by HEBs. They are arbitrarily divided into two forms: short-chain (SC, from 3 to ~300 Pi) and long-chain (LC, from 300 to ~1000 Pi), based on the method used for their extraction [98]. In trypanosomatids, the polyP has been proposed to be associated with several biological functions, such as osmoregulation [99], Ca<sup>2+</sup> signaling [100] and energy source storage [99]. Most polyPs in trypanosomatids are concentrated in acidocalcisomes [99], although polyP has also been found in the nucleus, cytosol and glycosomes. However, in BSF, polyPs have been detected mostly in acidocalcisomes and glycosomes [101]. PolyP is very abundant in BSF: 600 μM for LC and 250 μM for SC [102]). As the amount of polyP is measured by the molarity of phosphate units, these concentrations correspond to the number of monomers in the polymerized inorganic phosphates [103]. So, we consider LC+SC as the total

concentration of polyP corresponding to 850  $\mu\text{M}$ . Based on a cellular volume of 45  $\mu\text{m}^3$  per individual cell [30] (equivalent to 0.045 picoliters), the 850  $\mu\text{M}$  of Pi polymerized in polyP corresponds to  $\sim 38$  attomoles/cell. As each Pi corresponds to one HEB, which is equivalent to one ATP molecule, the total ATP required to synthesize the BSF's whole content of polyP is  $3.8 \times 10^{-17}$  mol of ATP, in other words,  $2.3 \times 10^7$  ATP molecules per parasite. Knocking out the Vacuolar Transporter Chaperone 4 in *T. brucei* caused a decrease of 25% of the total polyP [104]. As BSF are not challenged by strong osmolarity or nutritional variations (the main processes in which polyP are spent [104]) during their *in vitro* proliferation, we assume that this is the global rate of polyP degradation per cell cycle (5.3 h). Certainly, the ATP spent for polyP synthesis during the *in vivo* infection is higher since the parasites are subjected to blood osmolarity up to 1,400 mOsmol/l when they pass through the vasa recta of the mammalian kidney medulla [105], considerably higher than the  $\sim 300$  mOsmol/l in the global circulation [106]. It has been reported that hyperosmotic stress increases polyP synthesis [107]. During a cell cycle, BSF has to synthesize at least a new set of polyP for replication and renew the 25% of the polyP stock. Thus, the total ATP demand for synthesizing a new set of polyPs and maintaining the existing one is  $2.9 \times 10^7$  molecules. According to Liu et al., translocation of polyP across membranes is coupled to the polymerization of Pi and occurs without extra ATP cost [108]. We assumed that the total number of ATP molecules used for polyP synthesis (including its translocation from the cytosol into organelles) is equivalent to the total Pi units polymerized. This implies a total consumption of  $2.9 \times 10^7$  ATP molecules per cell cycle.

### Vitamins and other micronutrients

Trypanosomes also need vitamins and other micronutrients whose biosynthetic processes and/or uptake require ATP. Mechanisms for uptake from the medium have been identified for choline [109], pyridoxine (vitamin B6) [110] and riboflavin (vitamin B2) [111]. Ascorbic acid (vitamin C) biosynthesis has been identified in *T. brucei*, with the last step taking place within glycosomes [112]. Vitamin B1 is especially interesting because it is not efficiently taken up under physiological conditions suggesting that its intracellular levels must be obtained via biosynthesis [113]. Overall, considering the nutrients mentioned above, there is still much to be elucidated. Although there is evidence that biosynthesis occurs for some vitamins, such as B1 and B6, the pathways themselves are not understood in detail [110,113]. All works referenced in this section that identified an uptake mechanism for nutrients describe passive processes. Even if some of these compounds are biosynthesized, most of them are produced in low quantities. In summary, there is no evidence that these processes impact ATP levels meaningfully. Our conclusion for now, with some reservations, is that vitamin transport and biosynthesis do not have a significant impact on the energy budget of the parasite.

### ATP requirement for transmembrane transport

The cellular uptake of molecules and ions is part of the cell maintenance processes, and in most cases, it has an energy cost [15]. The energy dedicated to cell maintenance includes a contribution necessary for preserving a homeostatic ionic composition [114]. The energy demand by the uptake of amino acids, ammonium, potassium ions and inorganic phosphate from the extracellular medium into the cell was previously estimated for the synthesis of a new microbial cell, *in casu Escherichia coli* [13]. To obtain a value for the energy demand of BSF transport processes, we used the calculations made by Stouthamer as a model (Table 10). Stouthamer assumed that 0.5 moles of ATP are necessary for the uptake of 1 mole of  $\text{NH}_4^+$ , and 1 mole of ATP is necessary for the uptake of 1 mole of Pi, any amino acid, acetate or malate. For  $\text{Na}^+$  and  $\text{K}^+$  data are available for BSF *T. brucei*, allowing us to make a quite accurate calculation, and



**Table 10. ATP requirement for the formation of microbial cells from glucose and inorganic salts and the influence of the addition of amino acids (AA) or/and nucleic acid bases (bases). (Modified from [14]).**

Ion/Metabolite	ATP required (moles x 10 <sup>-4</sup> / g cells)		ATP required (moles x 10 <sup>-4</sup> / g cells)	
	AA	% of the total	AA + bases	% of the total
NH <sub>4</sub> <sup>+</sup>	10.4	3.0	0.0	0.0
Amino acids	47.9	13.7	47.9	15.3
Phosphate ions	7.7	2.2	7.7	2.5
<b>Total</b>	<b>66</b>	<b>18.9</b>	<b>55.6</b>	<b>17.7</b>

<https://doi.org/10.1371/journal.ppat.1011522.t010>

the cost of moving them across the plasma membrane was estimated separately (see below). It is worth mentioning that Stouthamer did not consider the costs of taking up glucose, which could be relevant for many prokaryotes but not for *T. brucei* where glucose transport happens by facilitated diffusion [115,116]. For *E. coli*, depending on the culture conditions, between 18.3 and 19.4% of the total energy required for a cell formation is needed only for overall solutes uptake [14]. Due to the lack of other data, we considered that BSF of *T. brucei* uses an intermediate percentage of its total ATP budget for solutes uptake (18.9%), representing  $\sim 1.1 \times 10^{11}$  ATP/cell cycle x cell. For the calculation of costs of the transport of Na<sup>+</sup> and K<sup>+</sup>, we used data previously obtained [117,118]. Considering that the ouabain-sensitive BSF Na<sup>+</sup>/K<sup>+</sup> ATPase has a specific activity for ATP hydrolysis of  $\sim 1.17$  nmoles/min x mg in which ATP is hydrolyzed into ADP + Pi with the concomitant exchange of 3 Na<sup>+</sup> for 2 K<sup>+</sup> [117,119], and that 1 mg of proteins is equivalent to 10<sup>8</sup> BSF cells [120], we calculated that a continuous activity of this pump during 5.3 hours would result in an ATP cost of  $2.2 \times 10^5$  ATP molecules per cell during an entire cell cycle. This value is negligible when compared to the total cost of transport of other ions and metabolites. Additionally, H<sup>+</sup>-ATPase is important to regulate the intracellular pH of BSF *T. brucei* and an approximate value of 534 nmol/min x mg protein was reported for the H<sup>+</sup> efflux [121]. Taking account of this value and the Stouthamer assumptions, we estimated that  $\sim 1.02 \times 10^{10}$  ATP molecules are necessary for the H<sup>+</sup> efflux per cell during an entire cell cycle. Several H<sup>+</sup>- and Ca<sup>2+</sup>-ATPases have been characterized at different levels of detail in BSF of *T. brucei*. For example, activities of both a V-H<sup>+</sup>-ATPase and a V-H<sup>+</sup>-PPase have been shown in acidocalcisomes [122,123], while V-H<sup>+</sup>-ATPase activities were also detected in the lysosome and endosomes, linking these pumps with endocytic processes [124]. In contrast, no evidence of a functional intracellular P-type H<sup>+</sup>-ATPase activity has been found in *T. brucei* [125]. However, despite their detailed description, we did not find enough data to estimate the costs related to these latter processes. Regarding Ca<sup>2+</sup> pumps, a high-affinity (Ca<sup>2+</sup>-Mg<sup>2+</sup>)-ATPase regulated by calmodulin was demonstrated in the plasma membrane of BSF trypanosomes, with a V<sub>max</sub> for ATP hydrolysis (in the presence of calmodulin) of 6.36 nmol/min x mg protein [126]. A continuous activity of this pump at maximum velocity during the entire BSF cell cycle (5.3 h, or 318 min) would demand 2,022 nmol ATP ( $\sim 1.22 \times 10^{18}$  ATP molecules). As 1 mg of proteins corresponds to 10<sup>8</sup> BSF cells, the maximum ATP demand by this pump per cell during an entire cell cycle is  $1.22 \times 10^{10}$  ATP molecules. However, this value is most likely an overestimation, because it is based on the assumption that this pump works at maximum velocity during the duration of the cell cycle. In addition, proteins with homology to PMCA-type Ca<sup>2+</sup>-ATPases were identified and reported in *T. brucei* as TbPMC1 and TbPMC2 [127]. In particular, TbPMC1 has been located in the plasma membrane of BSF. However, no information is available regarding its ATP consumption. Even so, we suggest that compared with the values estimated by Luo et al. [127], the ATP expenditure for Ca<sup>2+</sup> efflux could be negligible when compared to the total cost of transport processes in the parasite.

Based on these calculations, the estimated ATP costs for transport of solutes across the plasma membrane were estimated as being  $\sim 1.3 \times 10^{11}$  ATP/ cell cycle x cell.

### The cost of motility

Motility due to beating of its single flagellum serves the trypanosome to navigate the environment. But for BSF *T. brucei* it has the important additional role of counteracting the defense of the infected host, as it enables clearance of host antibodies attached to VSGs by causing these surface coat proteins to be recycled [128]. As a curiosity, the name *Trypanosoma* is derived from the Greek word describing the peculiar movement of these cells (auger cells) [129]. Trypanosomes are vigorous swimmers, and the swimming velocity depends on the microenvironment's viscosity. They can reach a speed of at least 20  $\mu\text{m/s}$ , allowing the hydrodynamic removal of attached host antibodies [130]. The frequency of flagellar beating has been measured as 15–20 Hz [131]. Considering that the resultant energy during the breakdown of 1 ATP molecule is  $\sim 7.5 \times 10^{-20}$  J and that the power generated by a flagellar beating is  $\sim 4 \times 10^{-17}$  J, one flagellar beating results from the consumption of at least 532 ATP molecules. If we assume that the ATP hydrolysis for flagellar motility is constant, based on the speed maintenance (output) and on the fact that trypanosomes are non-stopping engines, the total ATP consumed can be calculated as:

$$\text{ATP}_f = v \times N_{\text{ATP}} \times T$$

where  $\text{ATP}_f$  is the amount of ATP consumed by the flagellar movement during the entire BSF cell cycle,  $v$  is the frequency of flagellar beating (the average value of 17.5 Hz was taken for this calculation),  $N_{\text{ATP}}$  is the number of ATP molecules consumed per flagellar beating and  $T$  is the duration of the cell cycle in seconds. This calculation points out that permanent flagellar beating consumes  $2.3 \times 10^8$  ATP molecules per cell per cell cycle. This calculation does not yet take into account the specific characteristics of the internal flagellar machinery, which is responsible for transducing the energy obtained from ATP breakdown into flagellar beating. Inside a flagellum, the axoneme is constituted by 96 nm dynein repeats, forming two central double microtubules surrounded by nine other pairs of microtubules ( $9(2) + 2$ ) [132]. The basic dynein composition of each repeat is five outer arms (two-headed) and seven single-headed inner arms of dyneins [133]. Each dynein head has an AAA-ATPase domain [134], so in total, the axoneme has 17 ATPase domains at each 96 nm dynein repeat. As there are  $2 \times 9$  microtubules in a flagellum, there are a total of 306 ATPase domains/repeat. The average length of a BSF flagellum is 25.3  $\mu\text{m}$  [133], so dividing it by 96 nm, it is possible to calculate that a *T. brucei* flagellum has approximately 264 repeats with  $\sim 40,392$  dynein molecules. However, not all components of the flagellar machinery work at the same time. In order to generate a planar waveform, only some of the doublets are activated simultaneously, and the activity should switch periodically between two nearly-opposed doublets [135]. Considering that each beat is nearly planar in *T. brucei* BSF, instead of more than 40,392 dyneins operating at the same time, there will be those corresponding to 2 out of 9 pairs working simultaneously, in other words, 8,976 active dynein molecules per beat. To estimate the ATP consumption based on the dynein number, it must be considered that every single conformational change in dynein is driven by the formation of an ATP-dynein complex, which is before the power stroke. The power stroke is the motor force that drives the sliding displacement on the longitudinal axis of an axoneme [136]. The product of axonemal diameter and the shear angle (defined as the interior angle between the symmetry axis of the dynein head and the line tangent to the axoneme, immediately after the first bend), gives the total sliding displacement along an axoneme between two neighboring doublets [135,137]. For *Chlamydomonas*, it was

established that the shear angle is  $\sim 1$  rad. The diameter of an axoneme is  $\sim 150$  nm [138–140]. The dynein sliding displacement has been calculated as being 8 nm [136]. As a result, we have the ratio between the sliding displacement and the dynein power stroke, which results in 19 steps per flagellar beat. Assuming that each dynein takes 1 ATP per step, 8,976 of the dynein molecules being active at a given time, and that a flagellar beat needs 19 dynein steps along the microtubules, the parasite has to invest  $\sim 1.7 \times 10^5$  ATP molecules per flagellar beat. As previously stated, the average frequency for flagellar beating is 17.5 Hz. Remaking the calculation above with data from the mechanistic analysis of the flagellar machinery (see equation above) the ATP demand by the whole flagellar machinery would rise to  $5.7 \times 10^{10}$  molecules per cell cycle.

### ATP cost of activation and recruitment of vesicles

Endocytosis is a very important biological process in *T. brucei*, to capture specific compounds from the environment, such as low-density lipoprotein containing lipids and transferrin providing iron by the receptor-mediated process and serum proteins like albumin complexed with various molecules by fluid-phase endocytosis [90,141,142]. However, the mechanisms involved in this process have still not been fully described in this parasite [143]. The process is also crucial for the above-mentioned antibody clearance and VSG recycling which allows the trypanosome to escape from the host immune attack [144]. BSF possesses at least  $10^7$  VSG molecules per cell and recycles the entire VSG coat each 12 min [128]. To recycle VSGs, *T. brucei* depends on both endocytic and exocytic pathways. The VSGs are returned to the surface after passing through endosomes where any attached antibodies are removed and routed to the lysosomes for degradation. As every endocytic event in *T. brucei*, it depends on clathrin. For that, the cell produces 6–7 clathrin-coated vesicles bearing VSGs per second [145]. For our calculation, we used the minimum value of 6 clathrin-coated vesicles bearing VSGs per second, which implies that these cells would be internalizing 21,600 vesicles per hour. Vesicle formation for VSG recycling is a Rab11-dependent process [146]. Considering that the cell produces 21,600 vesicles per hour and at least 1 Rab assembly is necessary for each vesicle, the energy cost for the activation and recruitment of vesicles based on the assembly of Rab proteins (that use 1 GTP/Rab) results in a cost of  $1.14 \times 10^5$  GTP molecules per cell cycle. In this calculation, we are not taking into account some other processes that could impact endocytosis-related ATP consumption in *T. brucei*. Even though the endocytosis process is quite well understood in other organisms such as several opisthokonts [147], we are not able to estimate other ATP expenditures that can contribute to the total cost of endocytosis in *T. brucei* due to the low conservation of components for this machinery. For example, during the formation of the vesicles, several proteins are recruited to the site of membrane bending, and an actin bridge is built up [148]. The assembly of these proteins and the actin polymerization surrounding the vesicle involves ATP and GTP hydrolysis and/or cycling. For cargo translocation along tubulin microtubules, cycling of GTP is also necessary [149]. Clathrin and adaptor protein release also depends on ATPase activity [150]. Therefore, the minimal amount of ATP consumed for this process, considering a rate of conversion of 1 ATP per GTP is  $1.14 \times 10^5$  ATP molecules per cell cycle, but the actual number is probably higher.

### How much ATP hydrolysis is required to maintain the mitochondrial inner membrane potential ( $\Delta\Psi_m$ )?

The single mitochondrion of BSF *T. brucei* displays marked differences when compared to those of every other eukaryote described so far, and even when compared to that of other life cycle stages of the parasite, such as the procyclic form. The most remarkable differences are: i)

the absence of OxPhos; ii) a marked reduction in the expression levels of proton pumping respiratory enzyme complexes; and iii) a drastic reduction in the expression of TCA cycle enzymes [17]. It is worth mentioning that it could be reasonably assumed that in BSF trypanosomes the mitochondrial proton leakage is much smaller than that observed in other life stages [17], since the inner mitochondrial membrane does not form cristae, and therefore, it has a considerably smaller surface [151]. As the mitochondrial integrity and biogenesis depends on the mitochondrial inner membrane potential ( $\Delta\Psi_m$ ) [19,152], BSF compensates for the lack of functional respiratory proton pumps by using the  $F_1F_o$ -ATP-synthase in reverse mode [20]. In this way,  $\Delta\Psi_m$  is built up and maintained by pumping protons into the intermembrane space by hydrolysis of ATP [152]. Additionally, the cells require intramitochondrial ATP to prevent inhibition of the trypanosome alternative oxidase, which is needed to use oxygen as a terminal electron acceptor [153]. It must be noted that, the ATP required in the mitochondrial matrix to keep both systems working does not necessarily depend on ATP import via the ATP/ADP translocator [153]. In the absence of this transporter's activity, it can also rely on an intramitochondrial substrate-level phosphorylation system, comprising the acetate:succinate CoA transferase and the succinyl-CoA synthetase (ASCT/SCS) cycle [154]. This is reminiscent of the substrate-level phosphorylation and reversal of the ATP-synthase shown in other systems such as the isolated liver and heart rabbit mitochondria [155]. Such a system has been demonstrated as being functional in BSF in terms of intramitochondrial ATP production [156]. We hypothesize that this mitochondrial substrate-level phosphorylation system is the main source of intramitochondrial ATP, and it can provide sufficient ATP to maintain the  $\Delta\Psi_m$  [22,157], despite its relatively low capacity for producing only small quantities of ATP [10]. In terms of energy expenditure, the mitochondrial substrate-level phosphorylation could then be considered energetically neutral since all ATP produced by the ASCT/SCS cycle is devoted to the maintenance of the mitochondrial membrane potential generated by the  $F_1F_o$ -ATP synthase.

### Theoretical analysis of the ATP requirements for biomass formation and maintenance of BSF

The quantity of moles of ATP necessary to produce a gram of biomass (theoretical  $Y_{ATP}$ ) is an estimator of the ATP yield [158]. Several methods have been proposed to calculate its value. Here, we will assume that the total ATP produced during a cell cycle is used for maintenance and duplication, therefore we estimate it as:

$$Y_{ATP} = m / N_{ATP}^{Total}$$

where  $m$  is the dry weight of a single cell and  $N_{ATP}^{Total}$  is the total quantity of ATP used to maintain and duplicate a cell. The BSF dry weight is not available from the literature. Therefore, we estimated it from the value available for *E. coli*. Considering that the dry weight of an *E. coli* cell is 0.3 pg [159] and that its volume is  $1.3 \mu\text{m}^3$  [83], and assuming that the BSF of *T. brucei* with its volume of  $45 \mu\text{m}^3$  has the same density as the bacterium, we calculated a dry weight of approximately 10 pg/cell. Using this value and the total ATP produced during a cell cycle ( $6 \times 10^{11}$  ATP molecules/cell which equals  $0.99 \times 10^{-12}$  moles), and assuming that the total ATP produced is consumed, we obtained an  $Y_{ATP}$  of 10.1 (g biomass)/mole ATP. Another estimator of the efficiency of ATP used for biomass production (the ATP required for biomass duplication without considering the ATP required for maintenance) is the theoretical  $Y_{ATP}^{max}$ , which can be calculated as:

$$Y_{ATP}^{max} = m / N_{ATP}^{biomass}$$

where  $N_{ATP}^{biomass}$  is the quantity of ATP used for duplicating the biomass component of a cell

**Table 11. ATP produced during the cell cycle in different cells.**

Organism	Total	Reference
<i>Mycoplasma pneumoniae</i>	$4.3 \times 10^9$	[161]
<i>Escherichia coli</i>	$5.9\text{--}12 \times 10^9$	[13,162]
BSF <i>Trypanosoma brucei</i>	$5.94 \times 10^{11}$	This work
Mammalian tissue culture cell iBMK	$1.2 \times 10^{13}$	[163]
Human fibroblast	$4.5 \times 10^{13}$	[1]

<https://doi.org/10.1371/journal.ppat.1011522.t011>

[114], in our calculations  $2.1 \times 10^{11}$  ATP molecules or 0.35 pmoles ATP per cell. For the theoretical  $Y_{ATP}^{max}$  we then obtained a value of 28.6 (g biomass)/mole ATP.

## Discussion

Long-slender bloodstream forms of *T. brucei* have a unique configuration in terms of the bioenergetic pathways responsible for ATP production. Despite having a mitochondrion, these cells rely almost exclusively on glycolysis for ATP production, and they are the only case in nature (to the best of our knowledge) of mitochondriated cells in which the mitochondrion, under the conditions studied thus far, does not contribute to the cell's net ATP production. Even more, their ATP synthase hydrolyzes ATP to maintain the mitochondrial inner membrane potential [18,19,160]. Based on data available in the literature on the glycolytic flux during proliferation [12], we calculated with some precision the total amount of ATP produced during a BSF cell cycle, in other words, we calculated the ATP necessary for maintaining alive a BSF trypanosome and building a new one ( $\sim 6 \times 10^{11}$  molecules) when cultured in the rich HMI-9 medium.

When our numbers are compared with corresponding ones for other cells (Table 11), it becomes clear that, as expected, the ATP produced per cell during a cell cycle is much lower than that for other eukaryotes (mammalian cells), but much higher than that obtained for prokaryotic cells.

In order to expand our comparisons, we estimated the theoretical  $Y_{ATP}$  and  $Y_{ATP}^{max}$  of the *T. brucei* BSF, parameters that have previously been calculated for several other cells (Table 12). The obtained  $Y_{ATP}$  is 10.1 (g biomass)/mole ATP, higher than the value for *Saccharomyces*

**Table 12. Theoretical  $Y_{ATP}$  and  $Y_{ATP}^{max}$  for various cells.**

Organism	$Y_{ATP}$ (g biomass/mol ATP)	$Y_{ATP}^{max}$ (g biomass/mol ATP)	Reference
<i>Paracoccus denitrificans</i>	ND	$3.1\text{--}3.5^a$	[166]
<i>Escherichia coli</i>	ND	$16.7^\infty$	[167]
<i>Candida utilis</i>	ND	$20.8^b$	[164]
<i>Saccharomyces cerevisiae</i>	$15.8^c$	$28.1^b$	[164,168]
BSF <i>Trypanosoma brucei</i>	10.1	28.6	This work
<i>Sulfolobus solfataricus</i>	ND	$40.0^\infty$	[169]
<i>Corynebacterium glutamicum</i>	$34.5^{d*}$	ND	[170]

<sup>a</sup> autotrophic growth on formate

<sup>b</sup> aerobic glucose-limited chemostat growth

<sup>c</sup> anaerobic glucose-limited chemostat growth

<sup>d</sup> exponential growth on glucose

\* value corrected for the units used in this work

<sup>∞</sup> values derived from Growth Associated Maintenance (GAM) as follows:  $Y_{ATP}^{max} = 1/\text{GAM}$

<https://doi.org/10.1371/journal.ppat.1011522.t012>

*cerevisiae* (15.8 (g biomass)/mole ATP) [164]. Once knowing how much ATP is available for keeping alive and replicate a cell, it was interesting to analyze how much of this valuable resource is used for critical biological processes (Fig 1, S5 Table). The cost of DNA replication depends, in addition to the genome size, on the nucleotide composition and the specific ATP cost of their biosynthesis. Whilst in other organisms the average cost spent on dNTP biosynthesis from glucose is 50 ATP molecules [14], in *T. brucei* BSF it is only 10 ATP molecules. This is due to the fact that this parasite does not synthesize purines *de novo* but uses the salvage pathway, and synthesizes pyrimidines from externally supplied glutamine and aspartate. According to our calculations, 90% of the costs of the total DNA duplication is the cost of replicating the nuclear genome, while the remaining 10% corresponds to the cost of replicating the kDNA. Differently from replication, transcription costs are strongly influenced by other factors. Large polycistronic units are often assumed as costly because they involve the transcription of “useless” DNA (for example intergenic sequences, developmentally regulated genes, pseudogenes, *etc.*) that must be further eliminated during the *trans*-splicing processing for producing the mature mRNA, or by post-transcriptional degradation. However, according to our calculations, a significant part of the cost of transcription is due to the biosynthesis of rNTPs. As rNTP used in transcribing the intergenic regions can be recycled they would not constitute an extra cost [14]. So, the only extra cost that can be assumed is that of their polymerization (equivalent to 2 ATP/base). Considering this, the extra cost of polycistronic transcription is ~30% of the total transcriptional cost or 0.3% of the total budget for maintaining and building a new cell. There are not enough data to calculate in detail the total extra cost of transcribing coding sequences that must be further degraded in order to control gene expression. However, some estimations can be made based on the fact that only 47 out of 9,694 (~0.5%) genes are considered as not being expressed in BSF, and 772 out of 9,694 (8%) genes are considered down-regulated in BSF when compared to procyclic forms [165]. Considering the extreme case in which both gene populations are completely degraded after polymerization, the spurious coding RNA polymerization corresponds to 8.5% of the total coding RNAs. As we considered 2 ATP molecules being spent per base polymerized, an average transcript length of 2,800 nt, and an average RNA synthesis of 1.2 RNAs/h (estimated in [51]) the estimated ATP expenditure is  $\sim 2.9 \times 10^7$  ATP molecules (0.5% of the total ATP expenditure for the completion of a cell cycle) (Fig 1, S5 Table). These values can be compared with those that

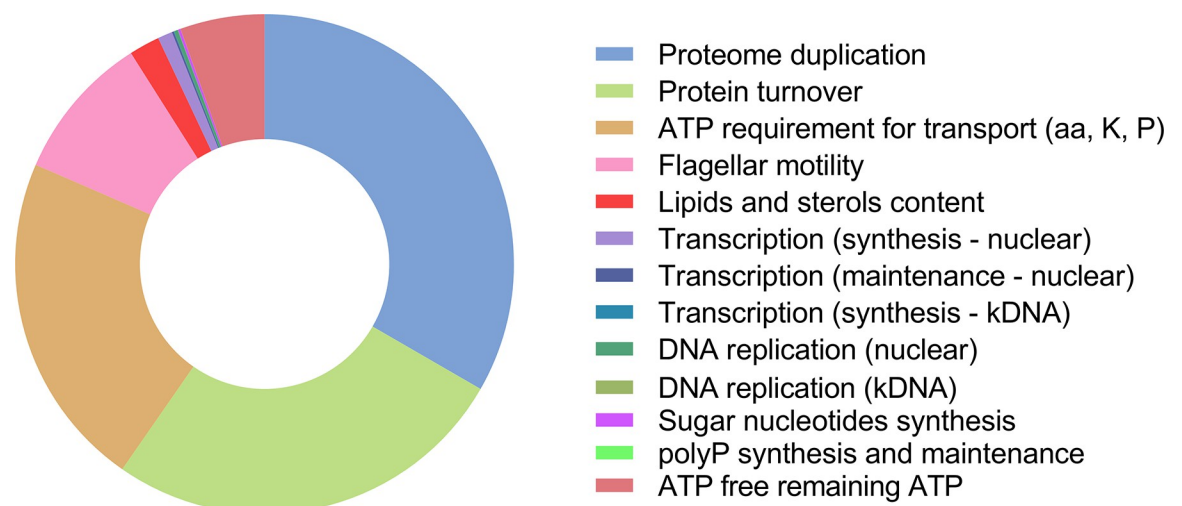


**Fig 1. Summary of the most energetically costly biological processes in bloodstream form *T. brucei*.** For underlying values see text and S5 Table.

<https://doi.org/10.1371/journal.ppat.1011522.g001>

can be estimated from a scenario of having transcriptional regulation for each protein-encoding gene. Considering that BSF expresses 8,875 genes this implies the formation of at least an equivalent number of transcriptional OCs, instead of the reduced number of OCs necessary in the polycistronic transcription system. Based on an individual cost of 20 ATP molecules/OC, the minimal cost of individual transcriptional initiation would be  $1.7 \times 10^5$  ATPs. We could as well estimate a maximum cost, by considering that each individual mRNA molecule requires ATP for formation of 1 OC. In this case, for the synthesis of the 37,988 mRNA molecules ( $N + Nr$ ) the ATP cost would be  $7.6 \times 10^5$  molecules. Thus, in both extreme hypothetical cases, a much higher value is obtained when transcriptional initiation is based on individual genes compared to the  $(0.8-1.5) \times 10^4$  ATPs required for OCs in the polycistronic transcription. Regardless of the case, both costs seem to be largely negligible concerning the total transcription cost and therefore from a purely energetic point of view the evolutionary advantage of individual transcription seems to be impactless.

As reported for several cell types, the synthesis and maintenance of the proteome is the most expensive process during a cell cycle (Tables S5 and 13). Despite the fact that BSF trypanosomes take up most of the amino acids from the medium instead of synthesizing them *de novo*, they are, according to our calculations, not an exception with regard to the expensiveness of proteome production and maintenance. This is explainable because the formation of peptide bonds is one of the costliest biochemical reactions in a cell (4 ATP molecules per bond). Therefore, taken together, translation and protein turnover demand 58.6% of the ATP budget (Fig 1). An interesting point emerges when analysing the cost of synthesizing the amino acids that compose the proteome in comparison with the energy required to import them from the environment. According to Mahmoudabadi, the average cost of synthesizing 1 amino acid is 2 ATPs [84]. We are assuming that during proteome turnover all amino acids are recycled. Thus, cost of synthesizing will only be considered for amino acids to be used for building a new proteome (not for maintenance involving turnover). We estimated that the synthesis of a new proteome demands  $4.7 \times 10^{10}$  amino acids. Therefore, the cost of synthesizing all amino acids would be  $9.4 \times 10^{10}$  ATPs. Herein we assumed that the total cost of uptake of amino acids

**Table 13. Comparison of ATP demand in different cell types.**

Process	ATP demand (%)		
	BSF <i>T. brucei</i> (This work)	Bacteria [13,171] <sup>a</sup>	Mammalian cells [172]
DNA replication	0.3	1.8	25 <sup>c</sup>
Transcription	1.1	11.8 <sup>b</sup>	
Proteome doubling	33.3	59.3 <sup>d</sup>	34 <sup>d</sup>
Protein turnover	26.3		
Sugar nucleotides synthesis	0.2	ND	ND
Lipids and sterols synthesis	2	0.3	ND
polyP synthesis and maintenance	0	ND	ND
Transport (aa, K <sup>+</sup> , Pi <sup>-</sup> )	21.8	18.1	33 <sup>e</sup>
Flagellar motility	9.5	ND	ND
Activation/recruitment of vesicles	0	ND	ND

<sup>a</sup> Bacteria grown in the presence of glucose, inorganic salts and amino acids

<sup>b</sup> Sum of RNA synthesis and turnover

<sup>c</sup> Sum of DNA/RNA synthesis

<sup>d</sup> Reference refers only to protein synthesis

<sup>e</sup> Sum of Na<sup>+</sup>/K<sup>+</sup> and Ca<sup>2+</sup> ATPases

ND, not determined

<https://doi.org/10.1371/journal.ppat.1011522.t013>

and ions was as estimated by Stouthamer for *E. coli* (between 13.7 and 15.3% of the total cell ATP budget). Taking the intermediate value of 14.5%, this would result in an ATP cost of  $8.6 \times 10^{10}$ , surprisingly very close to the cost estimated for amino acid biosynthesis. It is generally assumed that taking metabolites up is energetically more efficient than synthesizing them, and this efficiency would contribute to the parasitic lifestyle. Our calculations show that, in principle, for amino acids, the difference in *T. brucei* is very minor, impacting the total budget by less than 1.5%. These calculations do not include the cost of the synthesis of sugar nucleotides used for the glycosylation of surface proteins (mostly VSGs). Even being part of the total cost of building an entirely new proteome, it represents a negligible 0.5% of the total ATP demanded by this process.

Regarding the cost of synthesizing the lipidome, it is interesting to note that BSF trypanosomes contain most of the lipids commonly present in eukaryotic cells [173]. Although BSF *T. brucei* can acquire most of the lipids from the blood of the mammalian host [141], they have also the ability to rely completely on *de novo* biosynthesis of phospholipids and glycolipids to fulfill the need for some specific lipids [174]. For example, the VSG synthesis and anchoring in the plasma membrane requires high quantities of myristate, which is at low abundance in the host serum [175]. As most of the lipids biosynthesis pathways have been characterized in detail for *T. brucei* [94–97], we could estimate that the synthesis of the complete repertoire of lipids and sterols would consume 2% of the total ATP budget (Table 13, Fig 1). However, this value is likely to be an overestimation, since data indicate a balance between transport and biosynthesis is responsible for the maintenance of the lipids content in BSF *T. brucei* [89].

PolyPs are ubiquitously present among bacteria, protists and mammalian cells, and in unicellular eukaryotes have been proposed to have a role in different biological processes such as adaptation to stress, osmoregulation and metabolism regulation. In prokaryotes, they have been proposed as storage of HEbEs. Indeed, their hydrolysis involves the possibility of being coupled to phosphorylating ADP to ATP. However, based on our calculations, a role for polyPs as an energy reservoir seems unlikely: the total energy stored in the form of polyPs is less than 0.005% of the total ATP produced during a cell cycle (S6 Table) suggesting that their use as an energy reserve could only be restricted to very specific processes.

Regarding the costs of critical processes for survival and replication of BSF not related to the maintenance and duplication of biomass, we estimated the costs of motility, endo/exocytic vesicles formation, and the maintenance of the mitochondrial inner-membrane potential (which in the case of BSF is exclusively dependent on ATP hydrolysis). Motility occurs as a non-stop process during the entire cell cycle and is associated with the activity of the flagellar machinery. Two calculations were made on the basis of data available in the literature: i. based on the energy dissipated by the flagellar beating; and ii. based on the ATP demand of the flagellar structure, relying on the information on the composition and organization of the molecular motors responsible for the flagellar movement. Both calculations resulted in values differing by two orders of magnitude. It must be noted that both values refer to different phenomena since in the first case we estimated the energy output and in the second case the energy demand of the entire flagellar machinery. Therefore, if both values are correct, the efficiency of the machinery for flagellar beating can be calculated as the percentual ratio between the energy output and input, in this case approximately 0.5%. In this sense, it should be pointed out that Stellamanns et al. (2014) [131] found a discrepancy between the power necessary to move the BSF body in relation to the power actually produced by the flagellar movement in the range of one order of magnitude [131]. Whatever the case, the low efficiency of this process in terms of trypanosome motility is in agreement with the fact that flagellar beating is necessary for other processes not necessarily related to parasite movement, such as VSG recycling for antibody clearance [128,131]. To estimate the total percentage of the budget used for flagellar beating,



we considered the highest value obtained, which resulted in the consumption of 9.6% of ATP produced (Fig 1). Regarding the VSG recycling and antibody clearance, they require, in addition to flagellar movement, the formation of vesicles for trafficking the surface proteins through the cell interior. Due to the fact that the ATP (or in some cases GTP) requirements of these processes are largely unknown, we did not consider the cost of formation of the actin bridge, the cargo translocation along tubulin microtubules, and the clathrin and adaptor protein release [150]. Therefore, the ATP cost in our calculation is probably underestimated. However, as it represents less than approximately 0.0001%, the whole process is likely to be energetically undemanding.

Since BSF *T. brucei* is entirely dependent on glycolysis for its ATP supply, it is considered as an attractive drug target against sleeping sickness. Whether the quantitative analysis of the ATP consumption as presented in this paper can provide insight into which processes are most vulnerable for ATP depletion and responsible for killing the parasites is discussed in the S2 Text.

In this paper, we reported our calculation of the energy budget for maintaining alive and building up a BSF cell of *T. brucei* during its cell cycle based on the cellular and metabolic processes known to occur in these trypanosomes and data available about the ATP costs of the processes. Where relevant data for *T. brucei* were lacking, we estimated the costs based on data known for other organisms. Of course, the outcome of this endeavour is an approximation; for several processes in the trypanosomes, or even in general in cells, quantitative information is not available and/or how much ATP is required to sustain them is unknown (such processes are listed in the S3 Text). Nonetheless, the approximation seems realistic; all known major processes have been considered. Our analysis provided results that are amenable for experimental interrogation, while it also revealed where more research is required, including statistical analysis of the results, to allow an even more complete understanding of the energy expenditure of trypanosomes. Moreover, it will be interesting to expand this study to the analysis of other proliferative life-cycle stages of *T. brucei*, or those of related parasitic (e.g., the intracellular *T. cruzi* amastigote) and free-living organisms for which sufficient data are or may become available in the foreseeable future.

## Materials and methods

### Databases

**Methods.** (1) Our analysis is restricted to long-slender proliferating forms of BSF *T. brucei*. For their energy supply, these trypanosomes are entirely dependent on glucose uptake from the blood. Almost all glucose is converted to pyruvate, which is excreted, resulting in a yield of 2 ATP/glucose consumed. We have based our calculations on the quantitative analysis of the glucose consumption rate in exponentially growing trypanosomes of *T. brucei* strain Lister 427 with a doubling time of 5.3 h, in HMI-9 medium (composition described in S1 Table), as described by [12]. All calculations for rates of ATP consumption in different processes and activities of trypanosomes as described in the literature have been scaled to a cell cycle of 5.3 h.

(2) ATP consumption for biosynthetic processes has been calculated taking into account the (macro)molecular content (proteins, nucleic acids, lipids) of the trypanosomes, the known precursors which are either synthesized (according to available datasets in Table 14 and the reactions described in S2, S3 and S4 Tables) or taken up from the host environment, the rate of the processes and the turnover of the (macro)molecules. Also, the energy of uptake processes was considered.

(3) Other energy costs that were estimated involved: biogenesis of subcellular structures, endocytosis and recycling of the VSG surface coat, motility, protein degradation, and generation and maintenance of transmembrane electrochemical ion gradients.

**Table 14. Databases used in this work.**

Database	Web address	Reference
TriTrypDB	<a href="https://tritrypdb.org/tritrypdb/app">https://tritrypdb.org/tritrypdb/app</a>	[176]
Bionumbers	<a href="https://bionumbers.hms.harvard.edu/search.aspx">https://bionumbers.hms.harvard.edu/search.aspx</a>	[177]

<https://doi.org/10.1371/journal.ppat.1011522.t014>

**Detailed costs considered for each biological process.** Genome duplication: synthesis of deoxyribonucleotides (S2 Table), DNA unwinding, synthesis and ligation of Okasaki fragments and sliding clamp assembly.

Transcription: synthesis and polymerization of ribonucleotides (S3 Table), transcript length and half-life (rRNA, VSG, mRNA and SL RNA), nucleosome displacement, splicing.

Proteome maintenance: amino acid polymerization, protein half-life and degradation

Membrane doubling: synthesis of phospholipids and ergosterol

Synthesis of sugar nucleotides: average glucidic composition

Synthesis of polyphosphates: synthesis (with coupled transmembrane passage) of short-chain and long-chain polyP.

Transmembrane transport: transport of ions and amino acids (see S6 and S7 Tables and S3 Text))

Cell motility: flagellar beating, dynein sliding displacement and power stroke

Activation and recruitment of vesicles: rate of vesicle formation, Rab assembly

Maintenance of mitochondrial membrane potential: Fo-ATPase activity

Information about some of the processes listed here is very complete. However, for some other processes in the trypanosome major gaps exists in our knowledge, while for still other ones very little information is available. Where possible, quantitative information was taken from other organisms, or assumptions have been made. Where this has been done, it is mentioned in the text and tables.

## Supporting information

### S1 Table. Composition of HMI-9 and CMM.

(PDF)

### S2 Table. Reactions for synthesis of dNTPs.

(PDF)

### S3 Table. Reactions for synthesis of rNTPs.

(PDF)

### S4 Table. Reactions for synthesis of precursors of dNTPs and rNTPs.

(PDF)

### S5 Table. Summary of ATP production and expenditure in BSF trypanosomes.

(PDF)

### S6 Table. Amino acids transport and metabolic pathways in *T. brucei*.

(PDF)

### S7 Table. Calculations of synthesis flux for amino acids that can be produced from nutrients in CMM medium and their ATP flux.

(PDF)

### S1 Text. Biosynthesis of amino acids.

(PDF)

**S2 Text. What kills the BSF *T. brucei*?**

(PDF)

**S3 Text. Processes for which ATP costs could not be estimated due to lack of quantitative data.**

(PDF)

**Author Contributions****Conceptualization:** Paul A. M. Michels, Ariel M. Silber.**Data curation:** Janaina F. Nascimento, Paul A. M. Michels, Ariel M. Silber.**Formal analysis:** Janaina F. Nascimento, Rodolpho O. O. Souza, Mayke B. Alencar, Sabrina Marsiccobetre, Ana M. Murillo, Flávia S. Damasceno, Richard B. M. M. Girard, Letícia Marchese, Luis A. Luévano-Martinez, Renan W. Achjian, Jurgen R. Haanstra, Paul A. M. Michels, Ariel M. Silber.**Funding acquisition:** Janaina F. Nascimento, Ariel M. Silber.**Investigation:** Janaina F. Nascimento, Rodolpho O. O. Souza, Mayke B. Alencar, Sabrina Marsiccobetre, Ana M. Murillo, Flávia S. Damasceno, Richard B. M. M. Girard, Letícia Marchese, Luis A. Luévano-Martinez, Renan W. Achjian, Paul A. M. Michels, Ariel M. Silber.**Methodology:** Janaina F. Nascimento, Rodolpho O. O. Souza, Mayke B. Alencar, Sabrina Marsiccobetre, Ana M. Murillo, Flávia S. Damasceno, Richard B. M. M. Girard, Letícia Marchese, Luis A. Luévano-Martinez, Renan W. Achjian, Jurgen R. Haanstra, Paul A. M. Michels, Ariel M. Silber.**Project administration:** Janaina F. Nascimento.**Supervision:** Janaina F. Nascimento, Paul A. M. Michels, Ariel M. Silber.**Validation:** Janaina F. Nascimento, Rodolpho O. O. Souza, Mayke B. Alencar, Sabrina Marsiccobetre, Ana M. Murillo, Flávia S. Damasceno, Richard B. M. M. Girard, Letícia Marchese, Luis A. Luévano-Martinez, Renan W. Achjian, Paul A. M. Michels, Ariel M. Silber.**Visualization:** Rodolpho O. O. Souza, Mayke B. Alencar, Sabrina Marsiccobetre, Ana M. Murillo, Flávia S. Damasceno, Richard B. M. M. Girard, Letícia Marchese, Luis A. Luévano-Martinez, Renan W. Achjian, Paul A. M. Michels, Ariel M. Silber.**Writing – original draft:** Janaina F. Nascimento, Rodolpho O. O. Souza, Mayke B. Alencar, Sabrina Marsiccobetre, Ana M. Murillo, Flávia S. Damasceno, Richard B. M. M. Girard, Letícia Marchese, Luis A. Luévano-Martinez, Renan W. Achjian, Paul A. M. Michels, Ariel M. Silber.**Writing – review & editing:** Janaina F. Nascimento, Jurgen R. Haanstra, Paul A. M. Michels, Ariel M. Silber.**References**

1. Flamholz A, Phillips R, Milo R. The quantified cell. *Mol Biol Cell*. 2014; 25: 3497–3500. <https://doi.org/10.1091/mbc.E14-09-1347> PMID: 25368429
2. Gadelha C, Holden JM, Allison HC, Field MC. Specializations in a successful parasite: What makes the bloodstream-form African trypanosome so deadly? *Mol Biochem Parasitol*. 2011; 179: 51–58. <https://doi.org/10.1016/j.molbiopara.2011.06.006> PMID: 21763356

3. Lamour N, Riviere L, Coustou V, Coombs GH, Barrett MP, Bringaud FF. Proline metabolism in procyclic *Trypanosoma brucei* is down-regulated in the presence of glucose. *Journal of Biological Chemistry*. 2005; 280: 11902–11910. <https://doi.org/10.1074/jbc.M414274200> PMID: 15665328
4. Mantilla BS, Marchese L, Casas-Sánchez A, Dyer NA, Ejeh N, Biran M, et al. Proline metabolism is essential for *Trypanosoma brucei* survival in the tsetse vector. *PLoS Pathog*. 2017; 13: 1–29. <https://doi.org/10.1371/journal.ppat.1006158> PMID: 28114403
5. Rojas F, Silvester E, Young J, Milne R, Tettey M, Houston DR, et al. Oligopeptide signaling through TbGPR89 drives trypanosome quorum sensing. *Cell*. 2019; 176: 306–317.e16. <https://doi.org/10.1016/j.cell.2018.10.041> PMID: 30503212
6. Ryley JF. Studies on the metabolism of the protozoa. 9. Comparative metabolism of blood-stream and culture forms of *Trypanosoma rhodesiense*. *Biochem J*. 1962; 85: 211–23. <https://doi.org/10.1042/bj0850211> PMID: 13983265
7. Visser N, Opperdoes FR. Glycolysis in *Trypanosoma brucei*. *Eur J Biochem*. 1980; 103: 623–632. <https://doi.org/10.1111/j.1432-1033.1980.tb05988.x> PMID: 6766864
8. Hirumi H, Hirumi K. Continuous cultivation of *Trypanosoma brucei* bloodstream forms in a medium containing a low concentration of serum protein without feeder cell layers. *J Parasitol*. 1989; 75: 985. <https://doi.org/10.2307/3282883>
9. Creek DJ, Nijagal B, Kim DH, Rojas F, Matthews KR, Barrett MP. Metabolomics guides rational development of a simplified cell culture medium for drug screening against *Trypanosoma brucei*. *Antimicrob Agents Chemother*. 2013; 57: 2768–2779. <https://doi.org/10.1128/AAC.00044-13> PMID: 23571546
10. Michels PAM, Villafraz O, Pineda E, Alencar MB, Cáceres AJ, Silber AM, et al. Carbohydrate metabolism in trypanosomatids: New insights revealing novel complexity, diversity and species-unique features. *Exp Parasitol*. 2021; 224: 108102. <https://doi.org/10.1016/j.exppara.2021.108102> PMID: 33775649
11. Opperdoes FR, Borst P. Localization of nine glycolytic enzymes in a microbody-like organelle in *Trypanosoma brucei*. The glycosome. *FEBS Lett*. 1977; 80: 360–364. [https://doi.org/10.1016/0014-5793\(77\)80476-6](https://doi.org/10.1016/0014-5793(77)80476-6) PMID: 142663
12. Haanstra JR, van Tuijl A, van Dam J, van Winden W, Tielens AGM, van Hellemond JJ, et al. Proliferating bloodstream-form *Trypanosoma brucei* use a negligible part of consumed glucose for anabolic processes. *Int J Parasitol*. 2012; 42: 667–673. <https://doi.org/10.1016/j.ijpara.2012.04.009> PMID: 22580731
13. Stouthamer AH. A theoretical study on the amount of ATP required for synthesis of microbial cell material. *Antonie Van Leeuwenhoek*. 1973; 39: 545–565. <https://doi.org/10.1007/BF02578899> PMID: 4148026
14. Lynch M, Marinov GK. The bioenergetic costs of a gene. *Proc Natl Acad Sci U S A*. 2015; 112: 15690–15695. <https://doi.org/10.1073/pnas.1514974112> PMID: 26575626
15. Lynch M, Marinov GK. Membranes, energetics, and evolution across the prokaryote-eukaryote divide. *Elife*. 2017; 6: 1–30. <https://doi.org/10.7554/eLife.20437> PMID: 28300533
16. Helfert S, Estévez AM, Bakker B, Michels P, Clayton C. Roles of triosephosphate isomerase and aerobic metabolism in *Trypanosoma brucei*. *Biochemical Journal*. 2001; 357: 117. <https://doi.org/10.1042/0264-6021:3570117> PMID: 11415442
17. Zíková A, Verner Z, Nenarokova A, Michels PAM, Lukeš J. A paradigm shift: The mitoproteomes of procyclic and bloodstream *Trypanosoma brucei* are comparably complex. *PLoS Pathog*. 2017; 13: e1006679. <https://doi.org/10.1371/journal.ppat.1006679> PMID: 29267392
18. Nolan DP, Voorheis HP. The mitochondrion in bloodstream forms of *Trypanosoma brucei* is energized by the electrogenic pumping of protons catalysed by the F1F0-ATPase. *Eur J Biochem*. 1992; 209: 207–16. <https://doi.org/10.1111/j.1432-1033.1992.tb17278.x> PMID: 1327770
19. Schnauffer A, Clark-Walker GD, Steinberg AG, Stuart K. The F1-ATP synthase complex in bloodstream stage trypanosomes has an unusual and essential function. *EMBO J*. 2005; 24: 4029–40. <https://doi.org/10.1038/sj.emboj.7600862> PMID: 16270030
20. Vercesi AE, Docampo R, Moreno SNJ. Energization-dependent Ca<sup>2+</sup> accumulation in *Trypanosoma brucei* bloodstream and procyclic trypomastigotes mitochondria. *Mol Biochem Parasitol*. 1992; 56: 251–257. [https://doi.org/10.1016/0166-6851\(92\)90174-I](https://doi.org/10.1016/0166-6851(92)90174-I) PMID: 1484549
21. Opperdoes FR. Compartmentation of carbohydrate metabolism in trypanosomes. *Annu Rev Microbiol*. 1987; 41: 127–151. <https://doi.org/10.1146/annurev.mi.41.100187.001015> PMID: 3120638
22. Mochizuki K, Inaoka DK, Mazet M, Shiba T, Fukuda K, Kurasawa H, et al. The ASCT/SCS cycle fuels mitochondrial ATP and acetate production in *Trypanosoma brucei*. *Biochimica et Biophysica Acta (BBA)—Bioenergetics*. 2020; 1861: 148283. <https://doi.org/10.1016/j.bbabi.2020.148283> PMID: 32763239

23. Eisenthal R, Panes A. The aerobic/anaerobic transition of glucose metabolism in *Trypanosoma brucei*. FEBS Lett. 1985; 181: 23–27. [https://doi.org/10.1016/0014-5793\(85\)81106-6](https://doi.org/10.1016/0014-5793(85)81106-6) PMID: 3972106
24. Fairlamb AH, Opperdoes FR. Carbohydrate metabolism in African trypanosomes, with special reference to the glycosome. Carbohydrate Metabolism in Cultured Cells. Boston, MA: Springer US; 1986. pp. 183–224. [https://doi.org/10.1007/978-1-4684-7679-8\\_6](https://doi.org/10.1007/978-1-4684-7679-8_6)
25. Turnock DC, Ferguson MAJ. Sugar nucleotide pools of *Trypanosoma brucei*, *Trypanosoma cruzi*, and *Leishmania major*. Eukaryot Cell. 2007; 6: 1450–1463. <https://doi.org/10.1128/EC.00175-07> PMID: 17557881
26. Martin KL, Smith TK. The glycosylphosphatidylinositol (GPI) biosynthetic pathway of bloodstream-form *Trypanosoma brucei* is dependent on the *de novo* synthesis of inositol. Mol Microbiol. 2006; 61: 89–105. <https://doi.org/10.1111/j.1365-2958.2006.05216.x> PMID: 16824097
27. Mazet M, Morand P, Biran M, Bouysson G, Courtois P, Daulouède S, et al. Revisiting the central metabolism of the bloodstream forms of *Trypanosoma brucei*: production of acetate in the mitochondrion is essential for parasite viability. PLoS Negl Trop Dis. 2013; 7: e2587. <https://doi.org/10.1371/journal.pntd.0002587> PMID: 24367711
28. Creek DJ, Mazet M, Achcar F, Anderson J, Kim DH, Kamour R, et al. Probing the metabolic network in bloodstream-form *Trypanosoma brucei* using untargeted metabolomics with stable isotope labelled glucose. PLoS Pathog. 2015; 11: 1–25. <https://doi.org/10.1371/journal.ppat.1004689> PMID: 25775470
29. Graven P, Tambalo M, Scapozza L, Perozzo R. Purine metabolite and energy charge analysis of *Trypanosoma brucei* cells in different growth phases using an optimized ion-pair RP-HPLC/UV for the quantification of adenine and guanine pools. Exp Parasitol. 2014; 141: 28–38. <https://doi.org/10.1016/j.exppara.2014.03.006> PMID: 24657574
30. Rotureau B, Subota I, Bastin P. Molecular bases of cytoskeleton plasticity during the *Trypanosoma brucei* parasite cycle. Cell Microbiol. 2011; 13: 705–716. <https://doi.org/10.1111/j.1462-5822.2010.01566.x> PMID: 21159115
31. Berens RL, Marr JJ, LaFon SW, Nelson DJ. Purine metabolism in *Trypanosoma cruzi*. Mol Biochem Parasitol. 1981; 3: 187–196. [https://doi.org/10.1016/0166-6851\(81\)90049-9](https://doi.org/10.1016/0166-6851(81)90049-9) PMID: 6166862
32. Davies MJ, Ross AM, Gutteridge WE. The enzymes of purine salvage in *Trypanosoma cruzi*, *Trypanosoma brucei* and *Leishmania mexicana*. Parasitology. 1983; 87: 211–217. <https://doi.org/10.1017/S0031182000052574> PMID: 6316234
33. Tiwari K, Dubey VK. Fresh insights into the pyrimidine metabolism in the trypanosomatids. Parasit Vectors. 2018; 11: 1–15. <https://doi.org/10.1186/s13071-018-2660-8> PMID: 29422065
34. Berriman M, Ghedin E, Hertz-Fowler C, Blandin G, Renauld H, Bartholomeu DC, et al. The genome of the African trypanosome *Trypanosoma brucei*. Science. 2005; 309: 416–22. <https://doi.org/10.1126/science.1112642> PMID: 16020726
35. Ramanagoudr-Bhojappa R, Chib S, Byrd AK, Aarattuthodiyil S, Pandey M, Patel SS, et al. Yeast Pif1 helicase exhibits a one-base-pair stepping mechanism for unwinding duplex DNA. Journal of Biological Chemistry. 2013; 288: 16185–16195. <https://doi.org/10.1074/jbc.M113.470013> PMID: 23596008
36. Smith DJ, Whitehouse I. Intrinsic coupling of lagging-strand synthesis to chromatin assembly. Nature. 2012; 483: 434–438. <https://doi.org/10.1038/nature10895> PMID: 22419157
37. Majka J, Chung BY, Burgers PMJ. Requirement for ATP by the DNA damage checkpoint clamp loader. Journal of Biological Chemistry. 2004; 279: 20921–20926. <https://doi.org/10.1074/jbc.M400898200> PMID: 15014082
38. da Silva MS, Vitarelli MO, Souza BF, Elias MC. Comparative analysis of the minimum number of replication origins in trypanosomatids and yeasts. Genes (Basel). 2020; 11: 11–13. <https://doi.org/10.3390/genes11050523> PMID: 32397111
39. Melville SE, Leech V, Navarro M, Cross GAM. The molecular karyotype of the megabase chromosomes of *Trypanosoma brucei* stock 427. Mol Biochem Parasitol. 2000; 111: 261–273. [https://doi.org/10.1016/S0166-6851\(00\)00316-9](https://doi.org/10.1016/S0166-6851(00)00316-9) PMID: 11163435
40. Cooper S, Wadsworth ES, Ochsenreiter T, Ivens A, Savill NJ, Schnauffer A. Assembly and annotation of the mitochondrial minicircle genome of a differentiation-competent strain of *Trypanosoma brucei*. Nucleic Acids Res. 2019; 47: 11304–11325. <https://doi.org/10.1093/nar/gkz928> PMID: 31665448
41. Verner Z, Basu S, Benz C, Dixit S, Dobáková E, Faktorová D, et al. Malleable mitochondrion of *Trypanosoma brucei*. International Review of Cell and Molecular Biology. Elsevier Inc; 2015. <https://doi.org/10.1016/bs.ircmb.2014.11.001> PMID: 25708462
42. Jensen RE, Englund PT. Network news: The replication of kinetoplast DNA. Annu Rev Microbiol. 2012; 66: 473–491. <https://doi.org/10.1146/annurev-micro-092611-150057> PMID: 22994497

43. Johnson PJ, Kooter JM, Borst P. Inactivation of transcription by UV irradiation of *T. brucei* provides evidence for a multicistronic transcription unit including a VSG gene. *Cell*. 1987; 51: 273–281. [https://doi.org/10.1016/0092-8674\(87\)90154-1](https://doi.org/10.1016/0092-8674(87)90154-1) PMID: 3664637
44. Kooter JM, van der Spek HJ, Wagter R, d'Oliveira CE, van der Hoeven F, Johnson PJ, et al. The anatomy and transcription of a telomeric expression site for variant-specific surface antigens in *T. brucei*. *Cell*. 1987; 51: 261–272. [https://doi.org/10.1016/0092-8674\(87\)90153-X](https://doi.org/10.1016/0092-8674(87)90153-X) PMID: 2444341
45. Bernards A, Kooter JM, Borst P. Structure and transcription of a telomeric surface antigen gene of *Trypanosoma brucei*. *Mol Cell Biol*. 1985; 5: 545–553. <https://doi.org/10.1128/mcb.5.3.545-553.1985> PMID: 3879972
46. Gilinger G, Bellofatto V. Trypanosome spliced leader RNA genes contain the first identified RNA polymerase II gene promoter in these organisms. *Nucleic Acids Res*. 2001; 29: 1556–64. <https://doi.org/10.1093/nar/29.7.1556> PMID: 11266558
47. Günzl A, Bruderer T, Laufer G, Tu L, Chung H, Lee P, et al. RNA polymerase I transcribes procyclin genes and variant surface glycoprotein gene expression sites in *Trypanosoma brucei*. *Eukaryot Cell*. 2003; 2: 542–551. <https://doi.org/10.1128/EC.2.3.542>
48. Jäger A v, de Gaudenzi JG, Cassola A, D'Orso I, Frasch AC. mRNA maturation by two-step trans-splicing/polyadenylation processing in trypanosomes. *Proc Natl Acad Sci U S A*. 2007; 104: 2035–42. <https://doi.org/10.1073/pnas.0611125104> PMID: 17267594
49. Osinga KA, Swinkels BW, Gibson WC, Borst P, Veeneman GH, Van Boom JH, et al. Topogenesis of microbody enzymes: a sequence comparison of the genes for the glycosomal (microbody) and cytosolic phosphoglycerate kinases of *Trypanosoma brucei*. *EMBO J*. 1985; 4: 3811–3817. <https://doi.org/10.1002/j.1460-2075.1985.tb04152.x> PMID: 3004970
50. Gibson WC, Swinkels BW, Borst P. Post-transcriptional control of the differential expression of phosphoglycerate kinase genes in *Trypanosoma brucei*. *J Mol Biol*. 1988; 201: 315–325. [https://doi.org/10.1016/0022-2836\(88\)90140-4](https://doi.org/10.1016/0022-2836(88)90140-4) PMID: 2458474
51. Haanstra JR, Stewart M, Luu V-D, van Tuijl A, Westerhoff H V, Clayton C, et al. Control and regulation of gene expression: Quantitative analysis of the expression of phosphoglycerate kinase in blood-stream form *Trypanosoma brucei*. *Journal of Biological Chemistry*. 2008; 283: 2495–2507. <https://doi.org/10.1074/jbc.M705782200> PMID: 17991737
52. Boothroyd JC, Paynter CA, Coleman SL, Cross GAM. Complete nucleotide sequence of complementary DNA coding for a variant surface glycoprotein from *Trypanosoma brucei*. *J Mol Biol*. 1982; 157: 547–556. [https://doi.org/10.1016/0022-2836\(82\)90475-2](https://doi.org/10.1016/0022-2836(82)90475-2) PMID: 7120401
53. Müller LSM, Cosentino RO, Förstner KU, Guizetti J, Wedel C, Kaplan N, et al. Genome organization and DNA accessibility control antigenic variation in trypanosomes. *Nature*. 2018; 563: 121–125. <https://doi.org/10.1038/s41586-018-0619-8> PMID: 30333624
54. Michaeli S. *Trans*-splicing in trypanosomes: machinery and its impact on the parasite transcriptome. *Future Microbiol*. 2011; 6: 459–474. <https://doi.org/10.2217/fmb.11.20> PMID: 21526946
55. Stillman B. Histone modifications: insights into their influence on gene expression. *Cell*. 2018; 175: 6–9. <https://doi.org/10.1016/j.cell.2018.08.032> PMID: 30217360
56. Lowell JE, Kaiser F, Janzen CJ, Cross GAM. Histone H2AZ dimerizes with a novel variant H2B and is enriched at repetitive DNA in *Trypanosoma brucei*. *J Cell Sci*. 2005; 118: 5721–5730. <https://doi.org/10.1242/jcs.02688> PMID: 16303849
57. Siegel TN, Hekstra DR, Kemp LE, Figueiredo LM, Lowell JE, Fenyo D, et al. Four histone variants mark the boundaries of polycistronic transcription units in *Trypanosoma brucei*. *Genes Dev*. 2009; 23: 1063–1076. <https://doi.org/10.1101/gad.1790409> PMID: 19369410
58. Hecker H, Bender K, Betschart B, Modespacher UP. Instability of the nuclear chromatin of procyclic *Trypanosoma brucei brucei*. *Mol Biochem Parasitol*. 1989; 37: 225–234. [https://doi.org/10.1016/0166-6851\(89\)90154-0](https://doi.org/10.1016/0166-6851(89)90154-0) PMID: 2608098
59. Siegel TN, Hekstra DR, Wang X, Dewell S, Cross G a M. Genome-wide analysis of mRNA abundance in two life-cycle stages of *Trypanosoma brucei* and identification of splicing and polyadenylation sites. *Nucleic Acids Res*. 2010; 38: 4946–57. <https://doi.org/10.1093/nar/gkq237> PMID: 20385579
60. Matera AG, Wang Z. A day in the life of the spliceosome. *Nat Rev Mol Cell Biol*. 2014; 15: 108–121. <https://doi.org/10.1038/nrm3742> PMID: 24452469
61. Wang W, Carey M, Gralla JD. Polymerase II promoter activation: closed complex formation and ATP-driven start site opening. *Science* (1979). 1992; 255: 450–453. <https://doi.org/10.1126/science.1310361> PMID: 1310361
62. Yan M, Gralla JD. Multiple ATP-dependent steps in RNA polymerase II promoter melting and initiation. *EMBO Journal*. 1997; 16: 7457–7467. <https://doi.org/10.1093/emboj/16.24.7457> PMID: 9405374

63. Kolev NG, Franklin JB, Carmi S, Shi H, Michaeli S, Tschudi C. The transcriptome of the human pathogen *Trypanosoma brucei* at single-nucleotide resolution. *PLoS Pathog.* 2010; 6: 1–15. <https://doi.org/10.1371/journal.ppat.1001090> PMID: 20838601
64. Schulz D, Zaringhalam M, Papavasiliou FN, Kim HS. Base J and H3.V regulate transcriptional termination in *Trypanosoma brucei*. *PLoS Genet.* 2016; 12: 1–21. <https://doi.org/10.1371/journal.pgen.1005762> PMID: 26796638
65. Reynolds D, Hofmeister BT, Cliffe L, Alabady M, Siegel TN, Schmitz RJ, et al. Histone H3 variant regulates RNA polymerase II transcription termination and dual strand transcription of siRNA loci in *Trypanosoma brucei*. *PLoS Genet.* 2016; 12: e1005758. <https://doi.org/10.1371/journal.pgen.1005758> PMID: 26796527
66. Hsin JP, Manley JL. The RNA polymerase II CTD coordinates transcription and RNA processing. *Genes Dev.* 2012; 26: 2119–2137. <https://doi.org/10.1101/gad.200303.112> PMID: 23028141
67. Folkmann AW, Noble KN, Cole CN, Wente SR. Dbp5, Gle1-IP6 and Nup159: A working model for mRNP export. *Nucleus.* 2011; 2: 540–548. <https://doi.org/10.4161/nucl.2.6.17881> PMID: 22064466
68. Obado SO, Rout MP, Field MC. Sending the message: specialized RNA export mechanisms in trypanosomes. *Trends Parasitol.* 2022; 38: 854–867. <https://doi.org/10.1016/j.pt.2022.07.008> PMID: 36028415
69. Obado SO, Brillantes M, Uryu K, Zhang W, Ketaren NE, Chait BT, et al. Interactome mapping reveals the evolutionary history of the nuclear pore complex. *PLoS Biol.* 2016; 14: 1–30. <https://doi.org/10.1371/journal.pbio.1002365> PMID: 26891179
70. Ashkenazy-Titelman A, Atrash MK, Boocholez A, Kinor N, Shav-Tal Y. RNA export through the nuclear pore complex is directional. *Nat Commun.* 2022; 13: 5881. <https://doi.org/10.1038/s41467-022-33572-7> PMID: 36202822
71. Xie Y, Ren Y. Mechanisms of nuclear mRNA export: A structural perspective. *Traffic.* 2019; 20: 829–840. <https://doi.org/10.1111/tra.12691> PMID: 31513326
72. Kirby LE, Sun Y, Judah D, Nowak S, Koslowsky D. Analysis of the *Trypanosoma brucei* EATRO 164 bloodstream guide RNA transcriptome. *PLoS Negl Trop Dis.* 2016; 10: 1–18. <https://doi.org/10.1371/journal.pntd.0004793> PMID: 27399202
73. Koslowsky DJ, Yahampath G. Mitochondrial mRNA 3' cleavage/polyadenylation and RNA editing in *Trypanosoma brucei* are independent events. *Mol Biochem Parasitol.* 1997; 90: 81–94. [https://doi.org/10.1016/S0166-6851\(97\)00133-3](https://doi.org/10.1016/S0166-6851(97)00133-3) PMID: 9497034
74. Gazestani VH, Hampton M, Shaw AK, Salavati R, Zimmer SL. Tail characteristics of *Trypanosoma brucei* mitochondrial transcripts are developmentally altered in a transcript-specific manner. *Int J Parasitol.* 2018; 48: 179–189. <https://doi.org/10.1016/j.ijpara.2017.08.012> PMID: 29100810
75. Sement FM, Suematsu T, Zhang L, Yu T, Huang L, Aphasizheva I, et al. Transcription initiation defines kinetoplast RNA boundaries. *Proc Natl Acad Sci U S A.* 2018; 115: E10323–E10332. <https://doi.org/10.1073/pnas.1808981115> PMID: 30333188
76. Aphasizheva I, Alfonso J, Carnes J, Cestari I, Cruz-Reyes J, Göringer HU, et al. Lexis and grammar of mitochondrial RNA processing in Trypanosomes. *Trends Parasitol.* 2020; 36: 337–355. <https://doi.org/10.1016/j.pt.2020.01.006> PMID: 32191849
77. Read LK, Lukeš J, Hashimi H. Trypanosome RNA editing: the complexity of getting U in and taking U out. *WIREs RNA.* 2016; 7: 33–51. <https://doi.org/10.1002/wrna.1313> PMID: 26522170
78. Koslowsky D, Sun Y, Hindenach J, Theisen T, Lucas J. The insect-phase gRNA transcriptome in *Trypanosoma brucei*. *Nucleic Acids Res.* 2014; 42: 1873–1886. <https://doi.org/10.1093/nar/gkt973> PMID: 24174546
79. Aphasizhev R, Aphasizheva I. Mitochondrial RNA processing in trypanosomes. *Res Microbiol.* 2011; 162: 655–663. <https://doi.org/10.1016/j.resmic.2011.04.015> PMID: 21596134
80. Cooper S, Wadsworth ES, Schnauffer A, Savill NJ. Organization of minicircle cassettes and guide RNA genes in *Trypanosoma brucei*. *RNA.* 2022; 28: 972–992. <https://doi.org/10.1261/ma.079022.121> PMID: 35414587
81. Milo R. What is the total number of protein molecules per cell volume? A call to rethink some published values. *BioEssays.* 2013; 35: 1050–1055. <https://doi.org/10.1002/bies.201300066> PMID: 24114984
82. Albe KR, Butler MH, Wright BE. Cellular concentrations of enzymes and their substrates. *J Theor Biol.* 1990; 143: 163–195. [https://doi.org/10.1016/s0022-5193\(05\)80266-8](https://doi.org/10.1016/s0022-5193(05)80266-8) PMID: 2200929
83. Milo R, Phillips R. *Cell Biology by the Numbers*. Garland Science; 2015. <https://doi.org/10.1201/9780429258770>
84. Mahmoudabadi G, Phillips R, Lynch M, Milo R. Defining the energetic costs of cellular structures. *bioRxiv.* 2019; 1–14. <https://doi.org/10.1101/666040>

85. Peth A, Nathan JA, Goldberg AL. The ATP costs and time required to degrade ubiquitinated proteins by the 26 S proteasome. *Journal of Biological Chemistry*. 2013; 288: 29215–29222. <https://doi.org/10.1074/jbc.M113.482570> PMID: 23965995
86. Tinti M, Güther MLS, Crozier TWM, Lamond AI, Ferguson MAJ. Proteome turnover in the bloodstream and procyclic forms of *Trypanosoma brucei* measured by quantitative proteomics. *Wellcome Open Res*. 2019; 4: 1–26. <https://doi.org/10.12688/wellcomeopenres.15421.1> PMID: 31681858
87. Grünfelder CG, Engstler M, Weise F, Schwarz H, Stierhof Y-D, Boshart M, et al. Accumulation of a GPI-anchored protein at the cell surface requires sorting at multiple intracellular levels. *Traffic*. 2002; 3: 547–559. <https://doi.org/10.1034/j.1600-0854.2002.30805.x> PMID: 12121418
88. Paul KS, Jiang D, Morita YS, Englund PT. Fatty acid synthesis in African trypanosomes: a solution to the myristate mystery. *Trends Parasitol*. 2001; 17: 381–387. [https://doi.org/10.1016/s1471-4922\(01\)01984-5](https://doi.org/10.1016/s1471-4922(01)01984-5) PMID: 11685899
89. Poudyal NR, Paul KS. Fatty acid uptake in *Trypanosoma brucei*: Host resources and possible mechanisms. *Front Cell Infect Microbiol*. 2022; 12. <https://doi.org/10.3389/fcimb.2022.949409> PMID: 36478671
90. Coppens I, Levade T, Courtoy PJ. Host plasma low density lipoprotein particles as an essential source of lipids for the bloodstream forms of *Trypanosoma brucei*. *Journal of Biological Chemistry*. 1995; 270: 5736–5741. <https://doi.org/10.1074/jbc.270.11.5736> PMID: 7890701
91. Guan XL, Mäser P. Comparative sphingolipidomics of disease-causing trypanosomatids reveal unique lifecycle- and taxonomy-specific lipid chemistries. *Sci Rep*. 2017; 7: 1–13. <https://doi.org/10.1038/s41598-017-13931-x> PMID: 29051559
92. Richmond GS, Gibellini F, Young SA, Major L, Denton H, Lilley A, et al. Lipidomic analysis of bloodstream and procyclic form *Trypanosoma brucei*. *Parasitology*. 2010; 137: 1357–1392. <https://doi.org/10.1017/S0031182010000715> PMID: 20602846
93. Patnaik PK, Field MC, Menon AK, Cross GAM, Yee MC, Bütikofer P. Molecular species analysis of phospholipids from *Trypanosoma brucei* bloodstream and procyclic forms. *Mol Biochem Parasitol*. 1993; 58: 97–105. [https://doi.org/10.1016/0166-6851\(93\)90094-E](https://doi.org/10.1016/0166-6851(93)90094-E) PMID: 8459838
94. Dawoody Nejad L, Stumpe M, Rauch M, Hemphill A, Schneider R, Bütikofer P, et al. Mitochondrial sphingosine-1-phosphate lyase is essential for phosphatidylethanolamine synthesis and survival of *Trypanosoma brucei*. *Sci Rep*. 2020; 10: 1–11. <https://doi.org/10.1038/s41598-020-65248-x> PMID: 32427974
95. Lilley AC, Major L, Young S, Stark MJR, Smith TK. The essential roles of cytidine diphosphate-diacylglycerol synthase in bloodstream form *Trypanosoma brucei*. *Mol Microbiol*. 2014; 92: 453–470. <https://doi.org/10.1111/mmi.12553> PMID: 24533860
96. Lee SH, Stephens JL, Paul KS, Englund PT. Fatty acid synthesis by elongases in trypanosomes. *Cell*. 2006; 126: 691–699. <https://doi.org/10.1016/j.cell.2006.06.045> PMID: 16923389
97. Gibellini F, Hunter WN, Smith TK. Biochemical characterization of the initial steps of the Kennedy pathway in *Trypanosoma brucei*: The ethanolamine and choline kinases. *Biochemical Journal*. 2008; 415: 135–144. <https://doi.org/10.1042/BJ20080435> PMID: 18489261
98. Moreno SNJ, Docampo R. Polyphosphate and its diverse functions in host cells and pathogens. *PLoS Pathog*. 2013; 9: e1003230. <https://doi.org/10.1371/journal.ppat.1003230> PMID: 23658515
99. Docampo R, Ulrich P, Moreno SNJ. Evolution of acidocalcisomes and their role in polyphosphate storage and osmoregulation in eukaryotic microbes. *Philosophical Transactions of the Royal Society B: Biological Sciences*. 2010; 365: 775–784. <https://doi.org/10.1098/rstb.2009.0179> PMID: 20124344
100. Lander N, Cordeiro C, Huang G, Docampo R. Polyphosphate and acidocalcisomes. *Biochem Soc Trans*. 2016; 44: 1–6. <https://doi.org/10.1042/BST20150193> PMID: 26862180
101. Negreiros RS, Lander N, Huang G, Cordeiro CD, Smith SA, Morrissey JH, et al. Inorganic polyphosphate interacts with nucleolar and glycosomal proteins in trypanosomatids. *Mol Microbiol*. 2018; 110: 973–994. <https://doi.org/10.1111/mmi.14131> PMID: 30230089
102. Lemercier G, Espiau B, Ruiz FA, Vieira M, Luo S, Baltz T, et al. A pyrophosphatase regulating polyphosphate metabolism in acidocalcisomes is essential for *Trypanosoma brucei* virulence in mice. *Journal of Biological Chemistry*. 2004; 279: 3420–3425. <https://doi.org/10.1074/jbc.M309974200> PMID: 14615483
103. Cordeiro CD, Ahmed MA, Windle B, Docampo R. NUDIX hydrolases with inorganic polyphosphate exo- and endopolyphosphatase activities in the glycosome, cytosol and nucleus of *Trypanosoma brucei*. *Biosci Rep*. 2019; 39. <https://doi.org/10.1042/BSR20190894> PMID: 31043451
104. Lander N, Ulrich PN, Docampo R. *Trypanosoma brucei* vacuolar transporter chaperone 4 (TbVtc4) is an acidocalcisome polyphosphate kinase required for in vivo infection. *J Biol Chem*. 2013; 288: 34205–34216. <https://doi.org/10.1074/jbc.M113.518993> PMID: 24114837



105. Lang F. Mechanisms and significance of cell volume regulation. *J Am Coll Nutr.* 2007; 26: 613S–623S. <https://doi.org/10.1080/07315724.2007.10719667> PMID: 17921474
106. Meiselman HJ, Merrill EW, Gilliland ER, Pelletier GA, Salzman EW. Influence of plasma osmolarity on the rheology of human blood. *J Appl Physiol.* 1967; 22: 772–781. <https://doi.org/10.1152/jappl.1967.22.4.772> PMID: 6023192
107. Ruiz FA, Rodrigues CO, Docampo R. Rapid changes in polyphosphate content within acidocalcisomes in response to cell growth, differentiation, and environmental stress in *Trypanosoma cruzi*. *Journal of Biological Chemistry.* 2001; 276: 26114–26121. <https://doi.org/10.1074/jbc.M102402200> PMID: 11371561
108. Liu W, Wang J, Comte-Miserez V, Zhang M, Yu X, Chen Q, et al. Cryo-EM structure of the polyphosphate polymerase VTC reveals coupling of polymer synthesis to membrane transit. *EMBO J.* 2023; 42. <https://doi.org/10.15252/embj.2022113320> PMID: 37066886
109. Macêdo JP, Schmidt RS, Mäser P, Rentsch D, Vial HJ, Sigel E, et al. Characterization of choline uptake in *Trypanosoma brucei* procyclic and bloodstream forms. *Mol Biochem Parasitol.* 2013; 190: 16–22. <https://doi.org/10.1016/j.molbiopara.2013.05.007> PMID: 23747277
110. Gray A. *Trypanosoma brucei brucei*: Uptake and metabolism of pyridoxine and pyridoxal. *Exp Parasitol.* 1995; 80: 390–400. <https://doi.org/10.1006/expr.1995.1051> PMID: 7729474
111. Balcazar DE, Vanrell MC, Romano PS, Pereira CA, Goldbaum FA, Bonomi HR, et al. The superfamily keeps growing: Identification in trypanosomatids of RibJ, the first riboflavin transporter family in protists. *PLoS Negl Trop Dis.* 2017; 11: e0005513. <https://doi.org/10.1371/journal.pntd.0005513> PMID: 28406895
112. Wilkinson SR, Prathalingam SR, Taylor MC, Horn D, Kelly JM. Vitamin C biosynthesis in trypanosomes: a role for the glycosome. *Proc Natl Acad Sci U S A.* 2005; 102: 11645–50. <https://doi.org/10.1073/pnas.0504251102> PMID: 16087875
113. Stoffel SA, Rodenko B, Schweingruber AM, Mäser P, De Koning HP, Schweingruber ME. Biosynthesis and uptake of thiamine (vitamin B1) in bloodstream form *Trypanosoma brucei brucei* and interference of the vitamin with melarsen oxide activity. *Int J Parasitol.* 2006; 36: 229–236. <https://doi.org/10.1016/j.ijpara.2005.10.003> PMID: 16375907
114. Stouthamer AH, Bettenhausen C. Utilization of energy for growth and maintenance in continuous and batch cultures of microorganisms. *Biochimica et Biophysica Acta (BBA)—Reviews on Bioenergetics.* 1973; 301: 53–70. [https://doi.org/10.1016/0304-4173\(73\)90012-8](https://doi.org/10.1016/0304-4173(73)90012-8) PMID: 4574767
115. Ter Kuile BH, Opperdoes FR. Glucose uptake by *Trypanosoma brucei*. Rate-limiting steps in glycolysis and regulation of the glycolytic flux. *J Biol Chem.* 1991; 266: 857–62.
116. Gruenberg J, Sharma PR, Deshusses J. D-Glucose transport in *Trypanosoma brucei*: D-Glucose transport is the rate-limiting step of its metabolism. *Eur J Biochem.* 1978; 89: 461–9. <https://doi.org/10.1111/j.1432-1033.1978.tb12549.x> PMID: 710404
117. Nolan DP, Paul Voorheis H. Factors that determine the plasma-membrane potential in bloodstream forms of *Trypanosoma brucei*. *Eur J Biochem.* 2000; 267: 4615–4623. <https://doi.org/10.1046/j.1432-1327.2000.01477.x> PMID: 10903493
118. Bridges DJ, Pitt AR, Hanrahan O, Brennan K, Voorheis HP, Herzyk P, et al. Characterisation of the plasma membrane subproteome of bloodstream form *Trypanosoma brucei*. *Proteomics.* 2008; 8: 83–99. <https://doi.org/10.1002/pmic.200700607> PMID: 18095354
119. Van der Heyden N, Docampo R. Significant differences between procyclic and bloodstream forms of *Trypanosoma brucei* in the maintenance of their plasma membrane potential. *J Eukaryot Microbiol.* 2002; 49: 407–413. <https://doi.org/10.1111/j.1550-7408.2002.tb00220.x> PMID: 12425529
120. Opperdoes FR, Baudhuin P, Coppens I, De Roe C, Edwards SW, Weijers PJ, et al. Purification, morphometric analysis, and characterization of the glycosomes (microbodies) of the protozoan hemoflagellate *Trypanosoma brucei*. *Journal of Cell Biology.* 1984; 98: 1178–1184. <https://doi.org/10.1083/jcb.98.4.1178> PMID: 6715405
121. Vanderheyden N, Wong J, Docampo R. A pyruvate-proton symport and an H<sup>+</sup>-ATPase regulate the intracellular pH of *Trypanosoma brucei* at different stages of its life cycle. *Biochem J.* 2000; 346 Pt 1: 53–62. Available: <http://www.ncbi.nlm.nih.gov/pubmed/10657239>
122. Rodrigues CO, Scott DA, Docampo R. Characterization of a vacuolar pyrophosphatase in *Trypanosoma brucei* and its localization to acidocalcisomes. *Mol Cell Biol.* 1999; 19: 7712–7723. <https://doi.org/10.1128/MCB.19.11.7712> PMID: 10523660
123. Lemercier G, Dutoya S, Luo S, Ruiz FA, Rodrigues CO, Baltz T, et al. A vacuolar-type H<sup>+</sup>-pyrophosphatase governs maintenance of functional acidocalcisomes and growth of the insect and mammalian forms of *Trypanosoma brucei*. *Journal of Biological Chemistry.* 2002; 277: 37369–37376. <https://doi.org/10.1074/jbc.M204744200> PMID: 12121996

124. Huang G, Ulrich PN, Storey M, Johnson D, Tischer J, Tovar JA, et al. Proteomic analysis of the acidocalcisome, an organelle conserved from bacteria to human cells. *PLoS Pathog*. 2014; 10: e1004555. <https://doi.org/10.1371/journal.ppat.1004555> PMID: 25503798
125. Luo S, Fang J, Docampo R. Molecular characterization of *Trypanosoma brucei* P-type H<sup>+</sup>-ATPases. *Journal of Biological Chemistry*. 2006; 281: 21963–21973. <https://doi.org/10.1074/jbc.M601057200> PMID: 16757482
126. Benaim G, Lopez-Estraño C, Docampo R, Moreno SNJ. A calmodulin-stimulated Ca<sup>2+</sup> pump in plasma-membrane vesicles from *Trypanosoma brucei*; selective inhibition by pentamidine. *Biochemical Journal*. 1993; 296: 759–763. <https://doi.org/10.1042/bj2960759> PMID: 8280074
127. Luo S, Rohloff P, Cox J, Uyemura SA, Docampo R. *Trypanosoma brucei* plasma membrane-type Ca<sup>2+</sup>-ATPase 1 (TbPMC1) and 2 (TbPMC2) genes encode functional Ca<sup>2+</sup>-ATPases localized to the acidocalcisomes and plasma membrane, and essential for Ca<sup>2+</sup> homeostasis and growth. *Journal of Biological Chemistry*. 2004; 279: 14427–14439. <https://doi.org/10.1074/jbc.M309978200> PMID: 14724285
128. Engstler M, Pfohl T, Herminghaus S, Boshart M, Wiegertjes G, Heddergott N, et al. Hydrodynamic flow-mediated protein sorting on the cell surface of trypanosomes. *Cell*. 2007; 131: 505–515. <https://doi.org/10.1016/j.cell.2007.08.046> PMID: 17981118
129. Shimogawa MM, Ray SS, Kisalu N, Zhang Y, Geng Q, Ozcan A, et al. Parasite motility is critical for virulence of African trypanosomes. *Sci Rep*. 2018; 8: 9122. <https://doi.org/10.1038/s41598-018-27228-0> PMID: 29904094
130. Heddergott N, Krüger T, Babu SB, Wei A, Stellamanns E, Uppaluri S, et al. Trypanosome motion represents an adaptation to the crowded environment of the vertebrate bloodstream. *PLoS Pathog*. 2012; 8. <https://doi.org/10.1371/journal.ppat.1003023> PMID: 23166495
131. Stellamanns E, Uppaluri S, Hochstetter A, Heddergott N, Engstler M, Pfohl T. Optical trapping reveals propulsion forces, power generation and motility efficiency of the unicellular parasites *Trypanosoma brucei brucei*. *Sci Rep*. 2014; 4: 1–7. <https://doi.org/10.1038/srep06515> PMID: 25269514
132. Ralston KS, Hill KL. The flagellum of *Trypanosoma brucei*: new tricks from an old dog. *Int J Parasitol*. 2008; 38: 869–84. <https://doi.org/10.1016/j.ijpara.2008.03.003> PMID: 18472102
133. Imhof S, Zhang J, Wang H, Huy Bui K, Nguyen H, Atanasov I, et al. Cryo electron tomography with volta phase plate reveals novel structural foundations of the 96-nm axonemal repeat in the pathogen *Trypanosoma brucei*. *Elife*. 2019; 8: 1–30. <https://doi.org/10.7554/eLife.52058> PMID: 31710293
134. Trott L, Hafezparast M, Madzvamuse A. A mathematical understanding of how cytoplasmic dynein walks on microtubules. *R Soc Open Sci*. 2018; 5: 171568. <https://doi.org/10.1098/rsos.171568> PMID: 30224978
135. Chen DTN, Heymann M, Fraden S, Nicastro D, Dogic Z. ATP consumption of eukaryotic flagella measured at a single-cell level. *Biophys J*. 2015; 109: 2562–2573. <https://doi.org/10.1016/j.bpj.2015.11.003> PMID: 26682814
136. Lin J, Okada K, Raytchev M, Smith MC, Nicastro D. Structural mechanism of the dynein power stroke. *Nat Cell Biol*. 2014; 16: 479–85. <https://doi.org/10.1038/ncb2939> PMID: 24727830
137. Brokaw CJ. Direct measurements of sliding between outer doublet microtubules in swimming sperm flagella. *Science*. 1989; 243: 1593–6. <https://doi.org/10.1126/science.2928796> PMID: 2928796
138. Höög JL, Lacomble S, O'Toole ET, Hoenger A, McIntosh JR, Gull K. Modes of flagellar assembly in *Chlamydomonas reinhardtii* and *Trypanosoma brucei*. *Elife*. 2014; 3: 1–24. <https://doi.org/10.7554/elife.01479> PMID: 24448408
139. Bastin P, Pullen TJ, Moreira-Leite FF, Gull K. Inside and outside of the trypanosome flagellum: a multi-functional organelle. *Microbes Infect*. 2000; 2: 1865–74. [https://doi.org/10.1016/s1286-4579\(00\)01344-7](https://doi.org/10.1016/s1286-4579(00)01344-7) PMID: 11165931
140. Koyfman AY, Schmid MF, Gheiratmand L, Fu CJ, Khant HA, Huang D, et al. Structure of *Trypanosoma brucei* flagellum accounts for its bihelical motion. *Proc Natl Acad Sci U S A*. 2011; 108: 11105–8. <https://doi.org/10.1073/pnas.1103634108> PMID: 21690369
141. Coppens I, Baudhuin P, Opperdoes FR, Courtoy PJ. Receptors for the host low density lipoproteins on the hemoflagellate *Trypanosoma brucei*: purification and involvement in the growth of the parasite. *Proceedings of the National Academy of Sciences*. 1988; 85: 6753–6757. <https://doi.org/10.1073/pnas.85.18.6753> PMID: 3413122
142. Kariuki CK, Stijlemans B, Magez S. The trypanosomal transferrin receptor of *Trypanosoma brucei*—a review. *Trop Med Infect Dis*. 2019; 4. <https://doi.org/10.3390/tropicalmed4040126> PMID: 31581506
143. Link F, Borges AR, Jones NG, Engstler M. To the surface and back: exo- and endocytic pathways in *Trypanosoma brucei*. *Front Cell Dev Biol*. 2021; 9: 720521. <https://doi.org/10.3389/fcell.2021.720521> PMID: 34422837

144. Manna PT, Boehm C, Leung KF, Natesan SK, Field MC. Life and times: synthesis, trafficking, and evolution of VSG. *Trends Parasitol.* 2014; 30: 251–8. <https://doi.org/10.1016/j.pt.2014.03.004> PMID: 24731931
145. Engstler M, Thilo L, Weise F, Grünfelder CG, Schwarz H, Boshart M, et al. Kinetics of endocytosis and recycling of the GPI-anchored variant surface glycoprotein in *Trypanosoma brucei*. *J Cell Sci.* 2004; 117: 1105–1115. <https://doi.org/10.1242/jcs.00938> PMID: 14996937
146. Grünfelder CG, Engstler M, Weise F, Schwarz H, Stierhof Y-D, Morgan GW, et al. Endocytosis of a glycosylphosphatidylinositol-anchored protein via clathrin-coated vesicles, sorting by default in endosomes, and exocytosis via RAB11-positive carriers. *Mol Biol Cell.* 2003; 14: 2029–40. <https://doi.org/10.1091/mbc.e02-10-0640> PMID: 12802073
147. Adung'a VO, Gadelha C, Field MC. Proteomic analysis of clathrin interactions in trypanosomes reveals dynamic evolution of endocytosis. *Traffic.* 2013; 14: 440–57. <https://doi.org/10.1111/tra.12040> PMID: 23305527
148. Paraan M, Mendez J, Sharum S, Kurtin D, He H, Stagg SM. The structures of natively assembled clathrin-coated vesicles. *Sci Adv.* 2020; 6: eaba8397. <https://doi.org/10.1126/sciadv.aba8397> PMID: 32743076
149. Kaksonen M, Roux A. Mechanisms of clathrin-mediated endocytosis. *Nat Rev Mol Cell Biol.* 2018; 19: 313–326. <https://doi.org/10.1038/nrm.2017.132> PMID: 29410531
150. Hannan LA, Newmyer SL, Schmid SL. ATP- and cytosol-dependent release of adaptor proteins from clathrin-coated vesicles: A dual role for Hsc70. *Mol Biol Cell.* 1998; 9: 2217–29. <https://doi.org/10.1091/mbc.9.8.2217> PMID: 9693377
151. Bílý T, Sheikh S, Mallet A, Bastin P, Pérez-Morga D, Lukeš J, et al. Ultrastructural changes of the mitochondrion during the life cycle of *Trypanosoma brucei*. *Journal of Eukaryotic Microbiology.* 2021; 68. <https://doi.org/10.1111/jeu.12846> PMID: 33624359
152. Brown S V., Hosking P, Li J, Williams N. ATP synthase is responsible for maintaining mitochondrial membrane potential in bloodstream form *Trypanosoma brucei*. *Eukaryot Cell.* 2006; 5: 45–53. <https://doi.org/10.1128/EC.5.1.45-53.2006>
153. Peña-Díaz P, Pelosi L, Ebikeme C, Colasante C, Gao F, Bringaud F, et al. Functional characterization of TbMCP5, a conserved and essential ADP/ATP carrier present in the mitochondrion of the human pathogen *Trypanosoma brucei*. *Journal of Biological Chemistry.* 2012; 287: 41861–41874. <https://doi.org/10.1074/jbc.M112.404699> PMID: 23074217
154. Van Hellemond JJ, Opperdoes FR, Tielens AGM. Trypanosomatidae produce acetate via a mitochondrial acetate:succinate CoA transferase. *Proceedings of the National Academy of Sciences.* 1998; 95: 3036–3041. <https://doi.org/10.1073/pnas.95.6.3036> PMID: 9501211
155. Chinopoulos C, Gerencser AA, Mandi M, Mathe K, Töröcsik B, Doczi J, et al. Forward operation of adenine nucleotide translocase during  $F_0F_1$ -ATPase reversal: critical role of matrix substrate-level phosphorylation. *The FASEB Journal.* 2010; 24: 2405–2416. <https://doi.org/10.1096/fj.09-149898> PMID: 20207940
156. Jenkins TM, Eisenthal R, Weitzman PDJ. Two distinct succinate thiokinases in both bloodstream and procyclic forms of *Trypanosoma brucei*. *Biochem Biophys Res Commun.* 1988; 151: 257–261. [https://doi.org/10.1016/0006-291X\(88\)90587-6](https://doi.org/10.1016/0006-291X(88)90587-6) PMID: 3348777
157. Millerioux Y, Morand P, Biran M, Mazet M, Moreau P, Wargnies M, et al. ATP synthesis-coupled and -uncoupled acetate production from acetyl-CoA by mitochondrial acetate:Succinate CoA-transferase and acetyl-CoA thioesterase in *Trypanosoma*. *Journal of Biological Chemistry.* 2012; 287: 17186–17197. <https://doi.org/10.1074/jbc.M112.355404> PMID: 22474284
158. Bauchop T, Elsdén SR. The growth of micro-organisms in relation to their energy supply. *Microbiology (N Y).* 1960; 23: 457–469. <https://doi.org/10.1099/00221287-23-3-457> PMID: 13687855
159. Bakken LR, Olsen RA. Buoyant densities and dry-matter contents of microorganisms: conversion of a measured biovolume into biomass. *Appl Environ Microbiol.* 1983; 45: 1188–95. <https://doi.org/10.1128/aem.45.4.1188-1195.1983> PMID: 16346263
160. Panicucci B, Gahura O, Zíková A. *Trypanosoma brucei* TbIF1 inhibits the essential F1-ATPase in the infectious form of the parasite. *PLoS Negl Trop Dis.* 2017; 11: 1–21. <https://doi.org/10.1371/journal.pntd.0005552> PMID: 28414727
161. Wodke JAH, Puchalka J, Lluch-Senar M, Marcos J, Yus E, Godinho M, et al. Dissecting the energy metabolism in *Mycoplasma pneumoniae* through genome-scale metabolic modeling. *Mol Syst Biol.* 2013; 9: 653. <https://doi.org/10.1038/msb.2013.6> PMID: 23549481
162. Farmer IS, Jones CW. The energetics of *Escherichia coli* during aerobic growth in continuous culture. *Eur J Biochem.* 1976; 67: 115–122. <https://doi.org/10.1111/j.1432-1033.1976.tb10639.x> PMID: 786616

163. Fan J, Kamphorst JJ, Mathew R, Chung MK, White E, Shlomi T, et al. Glutamine-driven oxidative phosphorylation is a major ATP source in transformed mammalian cells in both normoxia and hypoxia. *Mol Syst Biol*. 2013; 9: 712. <https://doi.org/10.1038/msb.2013.65> PMID: 24301801
164. Verduyn C, Stouthamer AH, Scheffers WA, van Dijken JP. A theoretical evaluation of growth yields of yeasts. *Antonie Van Leeuwenhoek*. 1991; 59: 49–63. <https://doi.org/10.1007/BF00582119> PMID: 2059011
165. Naguleswaran A, Doiron N, Roditi I. RNA-Seq analysis validates the use of culture-derived *Trypanosoma brucei* and provides new markers for mammalian and insect life-cycle stages. *BMC Genomics*. 2018; 19: 227. <https://doi.org/10.1186/s12864-018-4600-6> PMID: 29606092
166. van Verseveld HW, Stouthamer AH. Growth yields and the efficiency of oxidative phosphorylation during autotrophic growth of *Paracoccus denitrificans* on methanol and formate. *Arch Microbiol*. 1978; 118: 21–26. <https://doi.org/10.1007/BF00406069> PMID: 211973
167. Feist AM, Henry CS, Reed JL, Krummenacker M, Joyce AR, Karp PD, et al. A genome-scale metabolic reconstruction for *Escherichia coli* K-12 MG1655 that accounts for 1260 ORFs and thermodynamic information. *Mol Syst Biol*. 2007; 3. <https://doi.org/10.1038/msb4100155> PMID: 17593909
168. Verduyn C, Postma E, Scheffers WA, Van Dijken JP. Energetics of *Saccharomyces cerevisiae* in anaerobic glucose-limited chemostat cultures. *J Gen Microbiol*. 1990; 136: 405–412. <https://doi.org/10.1099/00221287-136-3-405> PMID: 2202777
169. Ulas T, Riemer SA, Zaparty M, Siebers B, Schomburg D. Genome-Scale Reconstruction and Analysis of the Metabolic Network in the Hyperthermophilic Archaeon *Sulfolobus solfataricus*. *PLoS One*. 2012; 7. <https://doi.org/10.1371/journal.pone.0043401> PMID: 22952675
170. Coccagn-Bousquet M, Guyonvarch A, Lindley ND. Growth rate-dependent modulation of carbon flux through central metabolism and the kinetic consequences for glucose-limited chemostat cultures of *Corynebacterium glutamicum*. *Appl Environ Microbiol*. 1996; 62: 429–436. <https://doi.org/10.1128/aem.62.2.429-436.1996>
171. Russell JB, Cook GM. Energetics of bacterial growth: Balance of anabolic and catabolic reactions. *Microbiol Rev*. 1995; 59: 48–62. <https://doi.org/10.1128/mr.59.1.48-62.1995> PMID: 7708012
172. Buttgeriet F, Brand MD. A hierarchy of ATP-consuming processes in mammalian cells. *Biochemical Journal*. 1995; 312: 163–167. <https://doi.org/10.1042/bj3120163> PMID: 7492307
173. Carroll M, McCrorie P. Lipid composition of bloodstream forms of *Trypanosoma brucei brucei*. *Comparative Biochemistry and Physiology Part B: Comparative Biochemistry*. 1986; 83: 647–651. [https://doi.org/10.1016/0305-0491\(86\)90312-3](https://doi.org/10.1016/0305-0491(86)90312-3) PMID: 3956175
174. van Hellemond JJ, Tielens AGM. Adaptations in the lipid metabolism of the protozoan parasite *Trypanosoma brucei*. *FEBS Lett*. 2006; 580: 5552–5558. <https://doi.org/10.1016/j.febslet.2006.07.056> PMID: 16920110
175. Buxbaum LU, Milne KG, Werbovetz KA, Englund PT. Myristate exchange on the *Trypanosoma brucei* variant surface glycoprotein. *Proceedings of the National Academy of Sciences*. 1996; 93: 1178–1183. <https://doi.org/10.1073/pnas.93.3.1178> PMID: 8577736
176. Aslett M, Aurrecochea C, Berriman M, Brestelli J, Brunk BP, Carrington M, et al. TriTrypDB: a functional genomic resource for the Trypanosomatidae. *Nucleic Acids Res*. 2010; 38: D457–D462. <https://doi.org/10.1093/nar/gkp851> PMID: 19843604
177. Milo R, Jorgensen P, Moran U, Weber G, Springer M. BioNumbers—the database of key numbers in molecular and cell biology. *Nucleic Acids Res*. 2010; 38: D750–D753. <https://doi.org/10.1093/nar/gkp889> PMID: 19854939